Sites NGHP-01-21

By T. Collett, M. Riedel, J. Cochran, R. Boswell, J. Presley, P. Kumar, A. Sathe,
A. Sethi, M. Lall, and the National Gas Hydrate Program Expedition 01 Scientists

Scientific Investigations Report 2012–5054

U.S. Department of the Interior
U.S. Geological Survey

Contents

Figures

Tables

Site NGHP-01-21

By T. Collett, M. Riedel, J. Cochran, R. Boswell, J. Presley, P. Kumar, A. Sathe, A. Sethi, M. Lall, and the National Gas Hydrate Program Expedition 01 Scientists

Background and Objectives

Site NGHP-01-21 (Prospectus Site New FR1) is located at 15° 51.8531'N, 81° 50.0827'E in the Krishna-Godavari (KG) Basin (figs. 1 and 2). Water depth at Site NGHP-01-21 is at ~1,049 m. Site NGHP-01-21 is located near the industry well GD-3-1, which, along with Sites NGHP-01-10, NGHP-01-12, and NGHP-01-13, has previously shown strong evidence for highly concentrated gas hydrate deposits. In order to further delineate the gas-hydrate occurrence in and around the GD-3-1, Site NGHP-01-21 was established within the same seismically inferred disrupted area tested at Site NGHP-01-10. This site was also added at the end of the expedition to obtain additional gas-hydrate-bearing pressure-core samples for post-NGHP Expedition 01 study.

A high-resolution 2D seismic line (Line GDSW-16) is shown to illustrate the regional structural setting of Site NGHP-01-21 (figs. 2 and 3). The GDSW-16 seismic line shows a highly disrupted or faulted sedimentary sequence between the seafloor and deeper apparent high-amplitude gas occurrences. Individual reflectors can be traced for only a few hundred meters at most. A large-scale fault is identified on line GDSW-16 near shotpoint 600. Along line GDSW-16, the previously identified seismic inferred debris flow deposit is seen as a low-reflectivity unit in the immediate area surrounding Site NGHP-01-10.

Operations

This operations summary covers the Leg 4 DP move from Site NGHP-01-20 (KGGH05) to Site NGHP-01-21 (New Site FR1) and drilling/coring operations for Holes NGHP-01-21A through NGHP-01-21C (fig. 4). Schedule details and statistics for this site can be found as Appendixes:

- Appendix 1: NGHP Expedition 01 Operations Schedules
- Appendix 2: NGHP Expedition 01 Operations Statistics

Included in the Glossary is a list of standard or commonly used operations terms and acronyms.

Site NGHP-01-21 (New Site FR1) was a re-occupation of Site NGHP-01-10 (GD-3-1) drilled earlier on Leg 3A. It was designated with a new site number because the activities scheduled for this site were quite different than those designated for the original site. Site NGHP-01-10 provided the greatest opportunity for sampling gas hydrate during the expedition. Therefore, the site was re-occupied (as Site NGHP-01-21) to obtain additional samples of gas hydrate for preservation in the remaining dewars and pressure vessels. It was also an opportunity to recover additional cores under pressure using the FPC and HRC pressure-coring systems. There were no Pressure Core Sampler (PCS) deployments scheduled. Another final attempt at obtaining wireline logging data from below the BSR was also planned.

Hole NGHP-01-21A

Hole NGHP-01-21A was occupied on Leg 4 of NGHP Expedition 01 and was the first of what ultimately became three holes drilled at this site. The 3.3 NMI transit from Site NGHP-01-20 (KGGH05) was made in DP mode. The move took 1 hr at an average speed of 3.3 kt.

The vessel arrived at site NGHP-01-21A at 1722 hr 12 August. With the vessel above the site coordinates, a positioning beacon was deployed at 1740 hr. This site was located 20 m SE of Hole NGHP-01-10A on a bearing of 136°. The ice bath was installed in the moon pool and the same BHA as had been used on all previously cored sites was made up and deployed.

Hole NGHP-01-21A was planned to be drilled to ~50.0 mbsf followed by a series of three pressure-coring packages designed to target the massive gas-hydrate accumulation identified in the LWD/MWD logs and in earlier coring at Site NGHP-01-10. The pressure-coring packages were separated by two half-penetration XCB core deployments to provide the necessary tool turnaround time. These XCB cores also provided an opportunity to collect additional pressure vessel and liquid nitrogen samples, as well as samples for special shipboard experimentation. Half cores were designated because this has been proven as a more successful way to recover sediments laden with massive amounts of gas hydrates. By cutting half cores there is much more expansion space available within the core liner which leads to a much lower frequency of core “blowouts” and subsequent losses of core material.

The drill string was tripped to the seafloor and the top drive was picked up in preparation for spudding. Hole NGHP-01-21A was spudded at 1945 hr 12 August using an assumed sea-floor depth (based on Hole NGHP-01-10A) of

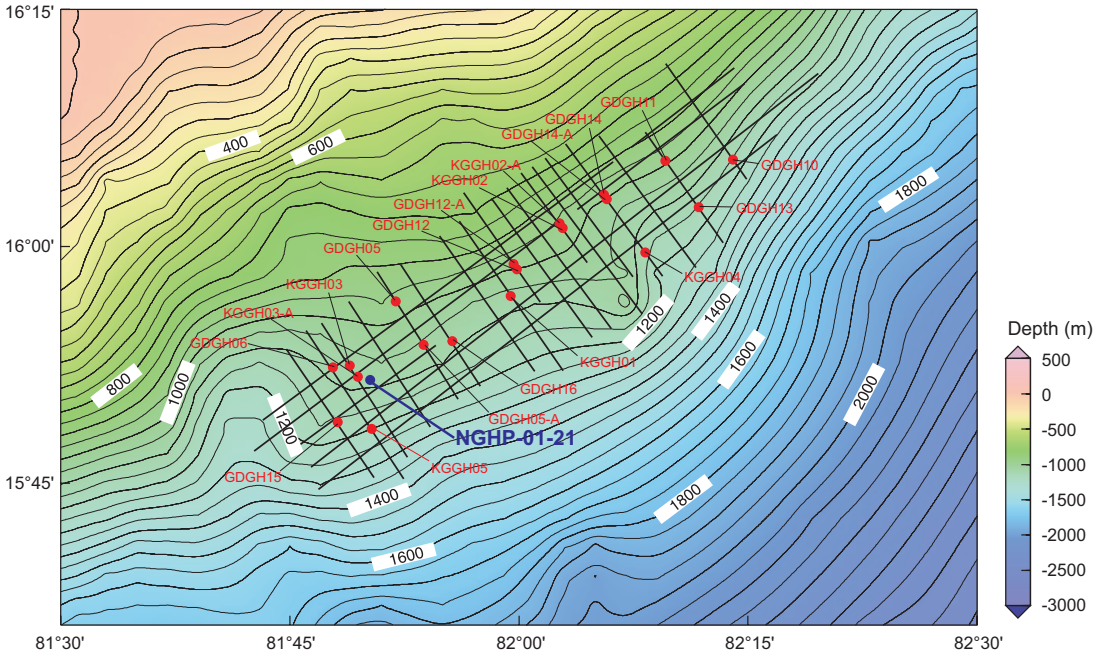

Figure 1. Bathymetric map of the Krishna-Godavari Basin with Site NGHP-01-21 (Prospectus Site New FR1).

1,049.0 mbrf. This was considered an accurate depth since the seafloor tag for Hole NGHP-01-10A (during the Leg 2 LWD/MWD drilling) was visually observed with the subsea TV camera. The PDR depth for this site, also taken from Hole NGHP-01-10A, was 1,055.4 mbrf.

Drilling with the XCB center bit continued to a depth of 48.4 mbsf where the center bit was recovered. The first XCB Core NGHP-01-21A-01X was then cut to a depth of 58.0 mbsf and this set up the first series of pressure-coring packages. FPC Core NGHP-01-21A-02Y was cut from 58.0 mbsf to 59.0 mbsf. This was followed by the first HRC Core NGHP-01-21A-03E which was cut from 59.0 mbsf to 60.0 mbsf. Two XCB half Cores NGHP-01-21A-04X and NGHP-01-21A-05X were then cut to a depth of 69.0 mbsf setting up the second series of pressure cores. FPC Core NGHP-01-21A-06Y was cut from 69.0 mbsf to 70.0 mbsf. This was followed by HRC Core NGHP-01-21A-07E which was cut from 70.0 mbsf to 71.0 mbsf. Two more XCB half Cores NGHP-01-21A-08X and NGHP-01-21A-09X were cut to a depth of 80.0 mbsf which set up the third and final series of pressure cores. FPC Core NGHP-01-21A-10Y was cut from 80.0 mbsf to 81.0 mbsf and this was followed by HRC Core NGHP-01-21A-11E cut from 81.0 mbsf to 82.0 mbsf. Coring was completed with two XCB half Cores NGHP-01-21A-12X and NGHP-01-21A-13X extending the hole to a total depth of 91.5 mbsf.

Penetration rates with the XCB ranged from 18.0 m/h to 38.4 m/h while core recovery ranged from 3 percent to 138 percent with an average for the hole of 67.5 percent.

Whirlpaks (containing microbeads), commonly used for assessing microbiological contamination, were not used. Accelerated core barrel handling protocols were used for all APC/XCB core barrels deployed in this hole. All core barrels were laid down immediately upon arrival at the rig floor before making another drill pipe connection or deploying the next core barrel.

For all HYACINTH pressure coring systems (FPC and HRC), a 15–20 min waiting period was used at the mudline on the way in the hole and again during retrieval. This was to cool the core barrels down and thus aid in keeping any entrained gas hydrate within the stability field. At the rig floor, all pressure core barrels (FPC and HRC) showing signs of proper actuation were placed in the moon pool ice bath prior to processing.

The hole was displaced with 30 bbl of 10.5 ppg Sepiolite mud and the drill string was pulled clear of the seafloor at 1525 hr 13 August. This completed operations in Hole NGHP-01-21A and initiated Hole NGHP-01-21B.

Hole NGHP-01-21B

Hole NGHP-01-21B was planned to have two pressure cores at ~55 mbsf and then to deepen to 200.0 mbsf for wireline logging. The depth of the pressure cores was selected to be within a gas-hydrate-rich interval and yet shallow enough that this portion of the hole would be stabilized behind the drill pipe during the wireline logging operation. Therefore, the condition of the hole for logging would not be compromised by the pressure-coring effort.

The vessel was offset 150 m SE of Hole NGHP-01-10A on a bearing of 136°. The top drive was picked up, the drill string spaced out, and hole NGHP-01-21B was spudded at 1620 hr 13 August. The PDR depth for this site, corrected to the rig floor DES, was 1,056.4 mbrf. This was 1.0 m deeper than the PDR depth for Hole NGHP-01-10A, so an assumed sea-floor depth of 1,050.0 mbrf.

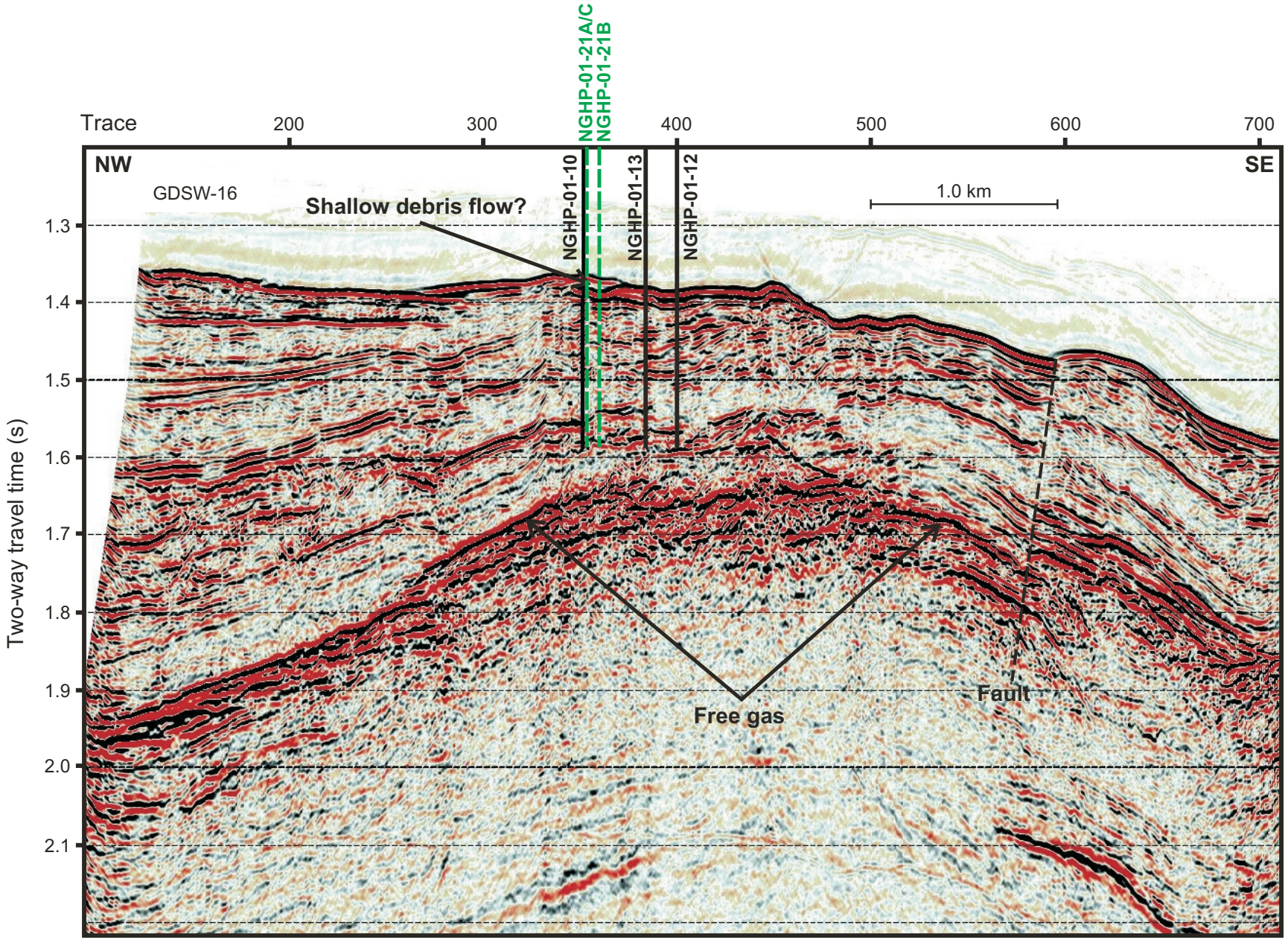

Figure 2. Seismic line GDSW-16 (orientation is NW-SE) crossing drill Site NGHP-01-21. Note the occurrence of deep-seated, high-amplitude reflectors indicating the occurrence of both free gas and a potential shallow debris flow.

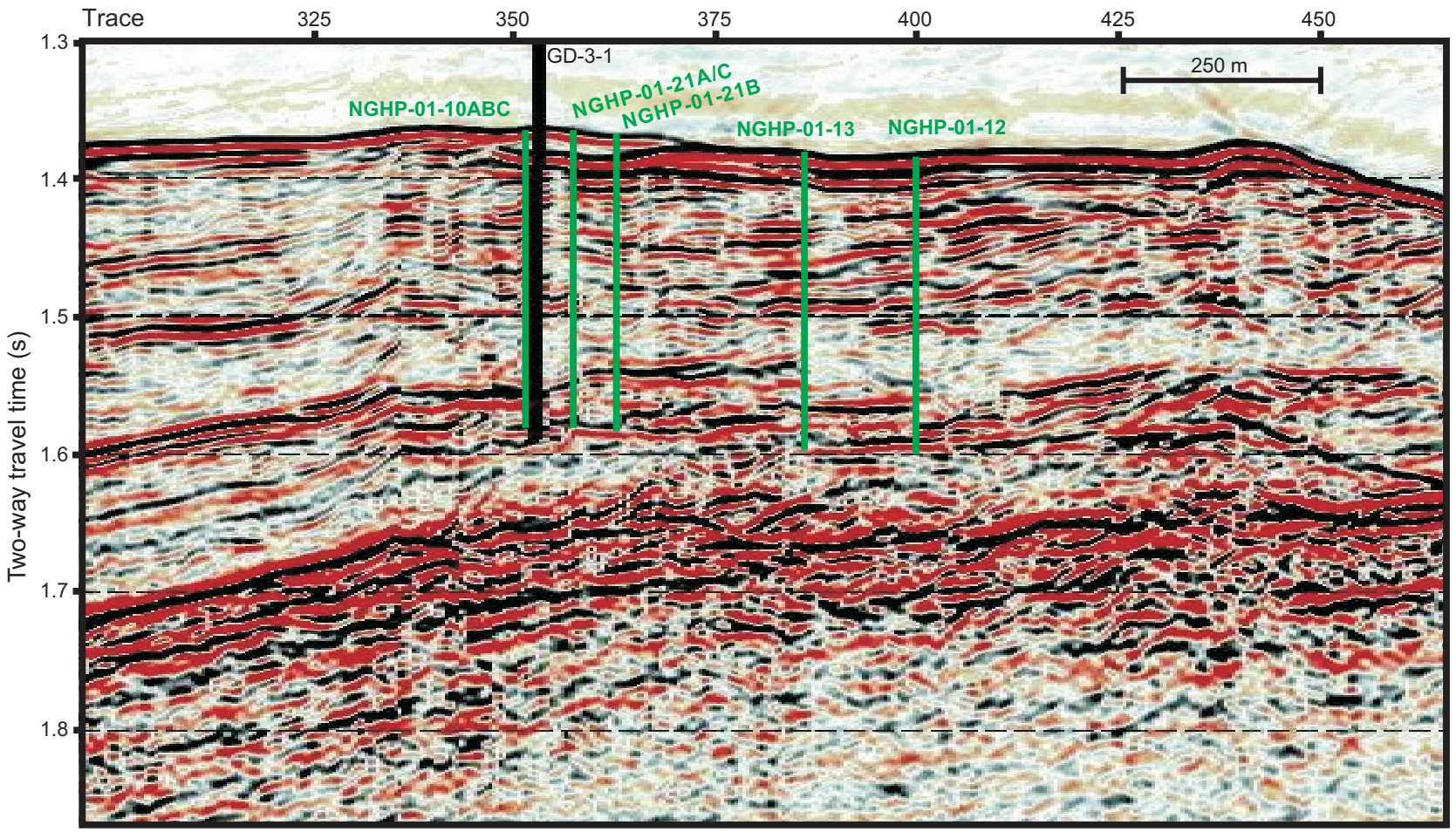

Figure 3. Enlargement of seismic line GDSW-16 showing the location of Sites NGHP-01-10, NGHP-01-12, NGHP-01-13, and NGHP-01-21.

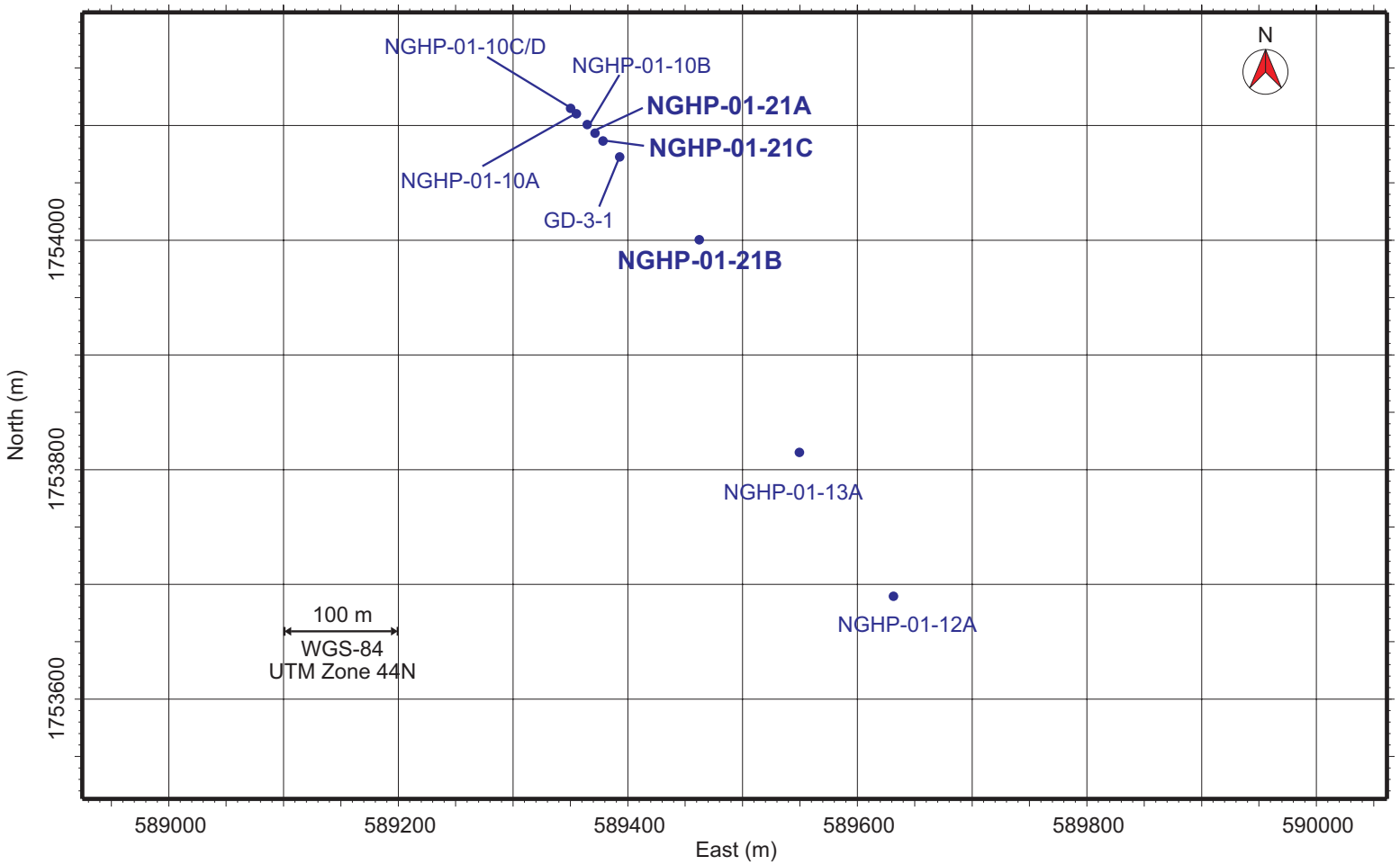

Figure 4. Map showing all holes occupied at Site NGHP-01-21 (New Site FR1).

Drilling with the XCB center bit continued to a depth of 55.0 mbsf where the center bit was recovered. Here, the first of two pressure cores was recovered. HRC Core NGHP-01-21B-01E was cut from 55.0 mbsf to 56.0 mbsf and FPC Core NGHP-01-21B-02Y was then cut from 56.0 mbsf to 57.0 mbsf.

For all HYACINTH pressure coring systems (FPC and HRC), a 15–20 min wait period was employed at the mudline on the way in the hole and again during retrieval. This was to cool the core barrels down and aid in keeping any entrained gas hydrate within the stability field. At the rig floor, the HRC barrel was placed in the moon pool ice bath prior to processing. The FPC failed to actuate correctly, recovering neither pressure nor core.

An XCB center bit was deployed and drilling then proceeded to a depth of 200.0 mbsf, where a Sepiolite mud sweep was pumped. The center bit was recovered and the hole was displaced with 60 bbls of 10.5 ppg mud in preparation for wireline logging. The top drive was racked after pulling one stand off of the bottom and the pipe trip then continued by placing the EOP at 58.3 mbsf.

At 0600 hr 14 August, rig-up for logging began. The first logging run was made with the triple combo tool suite. This suite of tools was unable to pass 101.0 mbsf. This was 99.0 m off the hole TD and ~74 m above the BSR. It was apparent that the logging tools would have to be deployed deeper in the hole to achieve the logging objectives. Therefore, the decision was made to log the interval from 101.0 m (~50 m), tie back the logging line and sheaves, and deploy the drill pipe to TD, clearing any bridges in the process. The pipe reached 155.0 mbsf before the top drive was required. The hole was then reamed to bottom and deepened by an additional 5.0 m to 205.0 mbsf to gain a bit more rat hole for the logging tools. This was to aid in recovering logging data from below and across the BSR (estimated at ~175 mbsf). The hole was flushed with a Sepiolite mud sweep, the center bit was recovered, and the hole was displaced a second time with 60 bbl of 10.5 ppg Sepiolite mud. This time the pipe was only pulled to a depth of 121.0 mbsf so as to allow logging of the lower portion of the hole first. Another episode of wireline logging was to be done later with the EOP raised back to the original 58.3 mbsf.

At 1600 hr 14 August, the logging line and sheaves were released from their tie-back position and the first logging run was made with the triple combo tool suite. Unfortunately, this tool string was unable to pass 160.0 mbsf; only 30 m beyond the bit and 15 m short of the BSR. All efforts to deploy the tool deeper were to no avail. During attempted recovery of the logging string, the tools became stuck in the hole. Several hours of selectively pumping, raising, lowering, and rotating the pipe was required before the tool eventually was worked free. In the process, all communication with the cable head was lost. In addition, much effort was expended to coax the tools through the flapper on the lockable float valve and into the drill string. Ultimately, the logging string was recovered back at the rig floor and 5 m of logging line directly above the cable head were found to be severely damaged with the outer armor completely stripped and tangled. Further logging efforts were abandoned, the Schlumberger logging sheaves were rigged down, and the drill string was pulled clear of the seafloor at 0030 hr 15 August. This completed operations in Hole NGHP-01-21B and began Hole NGHP-01-21C.

Hole NGHP-01-21C

Hole NGHP-01-21C was planned strictly as a shallow-pressure core hole using the limited operational time remaining to obtain a few final pressurized gas hydrate samples for preservation. No standard coring or wireline logging was scheduled. Two pressure cores with the FPC and two with the HRC were planned with a short drilled interval in between. The location of the pressure cores was once again selected to be within the gas-hydrate-rich interval located in the upper portion of the hole.

The vessel was offset 30 m SE of Hole NGHP-01-10A on a bearing of 136°. The top drive was picked up and the drill string spaced out just above an assumed seafloor depth of 1,049.0 mbrf. This seafloor was taken from Hole NGHP-01-21A which was only 10 m away. The pressure coring tools were prepared for deployment and Hole NGHP-01-21C was spudded at 0340 hr 15 August.

Drilling with the XCB center bit continued to a depth of 55.0 mbsf, where a 15-bbl Sepiolite mud sweep was circulated and the center bit was recovered. The first pressure core (FPC Core NGHP-01-21C-01Y) was cut from 55.0 mbsf to 56.0 mbsf. A short 0.5-m advance was used in cleaning up the rat hole from the FPC and the second pressure core (HRC Core NGHP-01-21C-02E) was cut from 56.5 mbsf to 57.5 mbsf.

An XCB center bit was used to advance the hole to a depth of 76.0 mbsf where another 15-bbl Sepiolite mud sweep was circulated out and the center bit was recovered. The third pressure core (FPC Core NGHP-01-21B-03Y) was cut from 76.0 mbsf to 77.0 mbsf and the final pressure core (HRC Core NGHP-01-21B-04E) was cut from 77.0 mbsf to a total hole depth of 78.0 mbsf.

For all HYACINTH pressure coring systems (FPC and HRC), a 15–20 min wait period was employed at the mudline on the way in the hole and again during retrieval. This was to cool the core barrels down and aid in keeping any entrained gas hydrate within the stability field. At the rig floor, all pressure core barrels were placed in the moon pool ice bath prior to processing.

The positioning beacon was recovered at 1744 hr during the pipe trip back to the surface. The BHA was disassembled, all drill collars were stored in the forward tubular rack, and the vessel was secured for transit. All thrusters and hydrophones were secured and at 2130 hr 15 August the vessel got underway at full speed for Chennai, India. This completed operations for Site NGHP-01-21 and also ended all on-site operations for Leg 4 of Expedition 01.

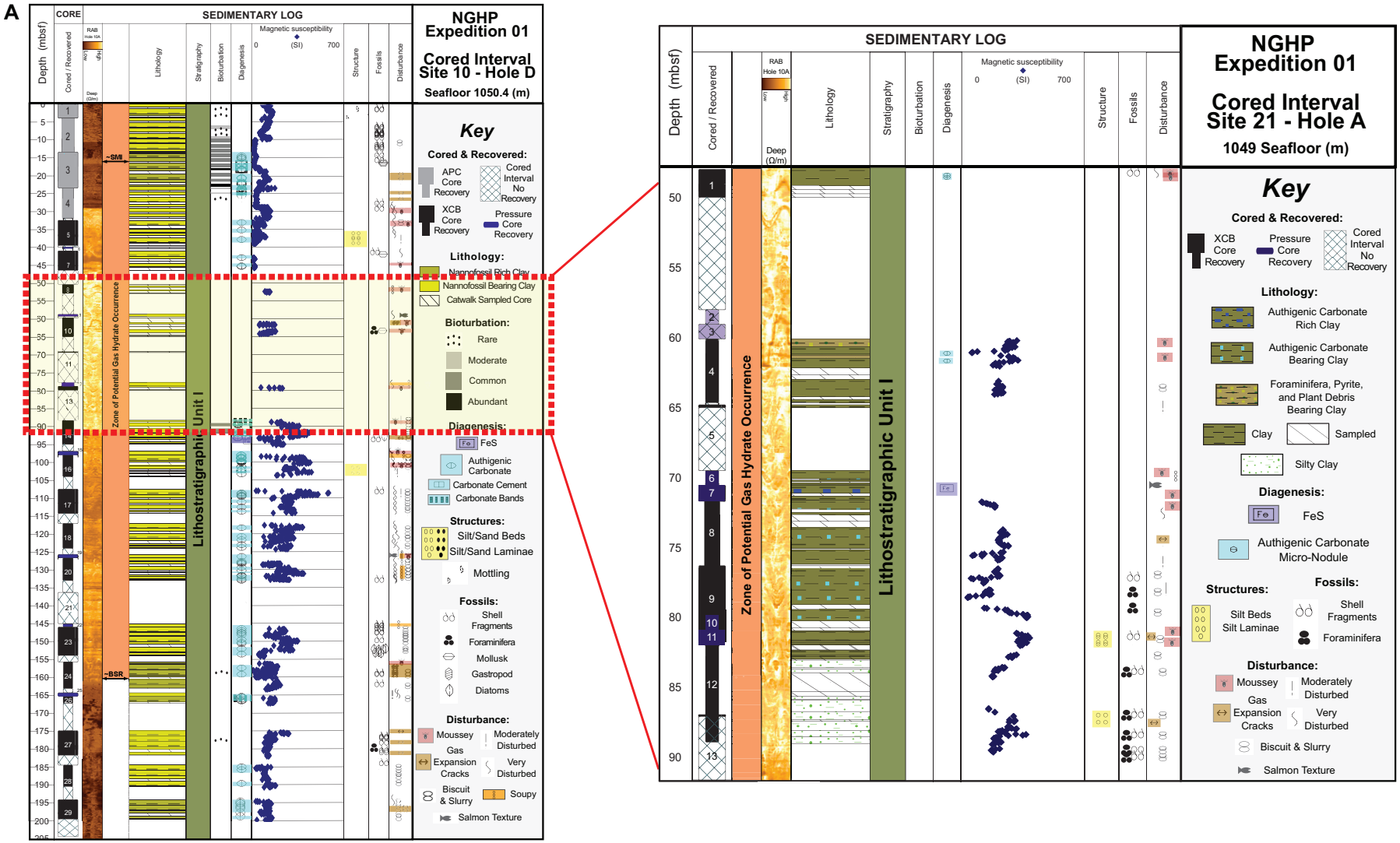

Figure 5. Lithostratigraphic summary of Hole NGHP-01-21A. A, The context: a comparison with Site NGHP-01-10; B, Site NGHP-01-21 summary alone. Note that colored intervals exceed symbol size when there is a range in the occurrence. The center point of each symbol represents the true depth of occurrence. Therefore, colored bars may slightly exceed core recovery; see Site NGHP-01-21 Visual Core Descriptions for the expanded scale and detailed core descriptions; see Site NGHP-01-21 Oversized Figures for the enlarged version of this summary. [BGHOZ, base of gas hydrate occurrence zone; RAB, resistivity at bit; SMI, sulfate-methane interface; BSR, bottom-simulating reflector]

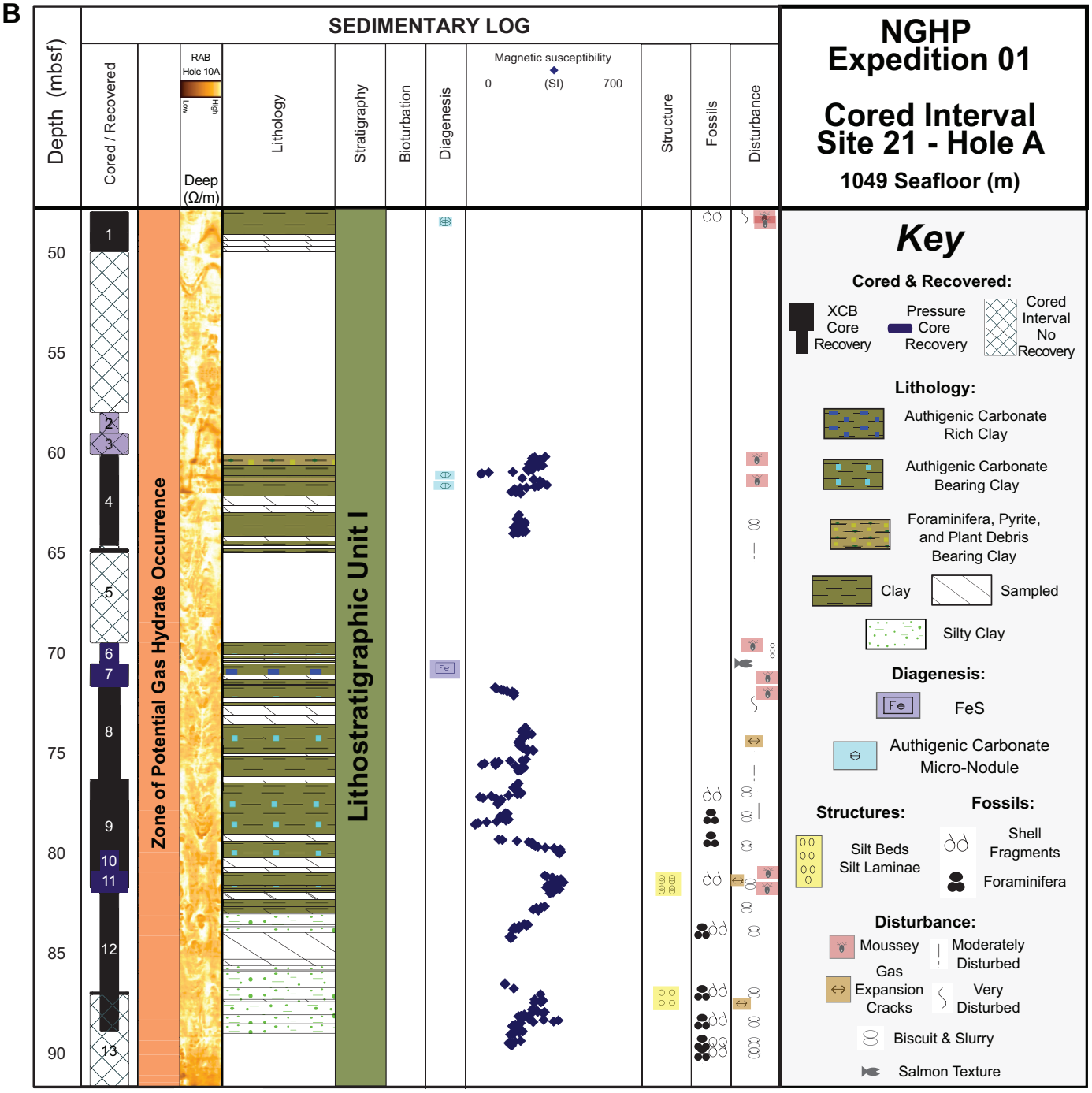

Figure 5. Lithostratigraphic summary of Hole NGHP-01-21A. A, The context: a comparison with Site NGHP-01-10; B, Site NGHP-01-21 summary alone. Note that colored intervals exceed symbol size when there is a range in the occurrence. The center point of each symbol represents the true depth of occurrence. Therefore, colored bars may slightly exceed core recovery; see Site NGHP-01-21 Visual Core Descriptions for the expanded scale and detailed core descriptions; see Site NGHP-01-21 Oversized Figures for the enlarged version of this summary. [BGHOZ, base of gas hydrate occurrence zone; RAB, resistivity at bit; SMI, sulfate-methane interface; BSR, bottom-simulating reflector]—Continued

Table 1. Smear-slide data for Hole NGHP-01-21A.

Sample reference		Mineral											
Core, section, depth (cm, in section)	MBSF	Quartz	Feld-spar	Mica	Heavy minerals	Volcanic glass	Pyrite	Iron sulfides	Fram-boidal pyrite	Rock frag-ments	Pumice	Other minerals	Authi-genic carbonates
NGHP-01-21A													
4X-1,65	60.65	trace			5		5						
4X-1,69	60.69				trace		5	5					
8X-3,80	73.7												
9X-6,36	81.84						50						
12X-5,75	85.87						70						

Lithostratigraphy

Site NGHP-01-21 is located in the KG Basin, along the eastern continental margin of India. The site was planned as a 150-m step-out to the SE from the location of gas hydrate-rich sediments recovered at sites NGHP-01-10 and NGHP-01-12. A total of three wells were drilled at Site NGHP-01-21 (see "Lithostratigraphy" and "Downhole Logging" in "Sites NGHP-01-10, 12, and 13"). Hole NGHP-01-21A was cored to a depth of 91.5 mbsf. Hole NGHP-01-21B was drilled to a total depth of 200 mbsf to further delineate the gas-hydrate accumulation at Sites NGHP-01-10 and NGHP-01-12 through coring, pressure coring, and wireline logging. Hole NGHP-01-21C was dedicated to gas-hydrate sample collection with pressure coring and was drilled to a depth of 78 mbsf. Of these holes, only cores from Hole NGHP-01-21A have been described for lithostratigraphy in the sedimentology lab.

The sedimentary sequence recovered at Site NGHP-01-21 is classified as a single lithostratigraphic unit (that is, Lithostratigraphic Unit I; fig. 5B). As at other sites, the classification is based on sedimentological criteria (for example, variations in sedimentary structure and grain size or biogenic and lithologic components) and other parameters (fig. 5B, table 1, and Site NGHP-01-21 Visual Core Descriptions). We also analyze our results in the context of physical property measurements (for example, magnetic susceptibility) to better understand sedimentation characteristics at Site NGHP-01-21 (see "Operations").

The lack of *Discoaster spp*. at this site also leads us to suspect that the stratigraphy recovered at Site NGHP-01-20 is Quaternary in age and may be equivalent to the uppermost KG-Basin stratigraphy recovered at other sites

Lithostratigraphic Units

Lithostratigraphic Unit I

Intervals: Hole NGHP-01-21A, Sections NGHP-01-21A-01X-01 to NGHP-01-21A-13X-CC (TD)

Depth: Hole NGHP-01-21A, 48-91.5 mbsf

Age: Quaternary

The XCB cores were advanced at 5-m increments, which resulted in good recovery at Site NGHP-01-21 compared to the same depth interval at Sites NGHP-01-10 and NGHP-01-12 (see "Lithostratigraphy" in "Sites NGHP-01-10, 12 and 13"). Lithostratigraphic Unit I is composed of clays with modifiers in the top ~37 m of the cored interval (that is, authigenic carbonate and thin intervals with foraminifera, pyrite, and plant debris). Sediments are primarily black (10YR 2.5/1; 2.5Y 2.5/1) and gray (5GY 3/1; N/3) with an occasional thin grayish brown interval (2.5 Y 4/2). As at Sites NGHP-01-10 and NGHP-01-12, clays contain significant terrigenous organic matter that is visible in smear slides (table 1). Silt laminae and beds are rare at Site NGHP-01-21, although the amount of silt is consistently high and zones with high silt are commonly seen on the surface of the cores (fig. 6), especially at the bottom of the hole, where silty clays were recovered.

Mollusk shell fragments and rare visible foraminifera tests occur sporadically throughout the stratigraphy at the visual level as well as in the processed coarse fraction (table 2). The total biogenic component of the sediment is a mixture of calcareous nannofossils, foraminifera, and plant debris found at comparatively low levels (less than 5 percent individually) relative to Sites NGHP-01-10 and NGHP-01-12 (table 1; fig. 7). The major non-biogenic components of Lithostratigraphic Unit I are clays, quartz, authigenic carbonates and iron sulfides (table 1). Whereas authigenic carbonate is consistently high at a microscopic scale (in smear slides), the number of authigenic carbonate nodules (only micro-nodules; fig. 5) is greatly reduced compared to sediments above and below this level at Sites NGHP-01-10 and NGHP-01-12. Downcore magnetic susceptibility measurements (fig. 5) are at similar levels as in Sites NGHP-01-10 and NGHP-01-12 and a similar degree of variability, suggesting that both primary and secondary diagenetic magnetic minerals should be taken in account when interpreting the data.

Sediments recovered in Hole NGHP-01-21A are located in the low recovery zone of Sites NGHP-01-10 and NGHP-01-12 (that is, 45 to 88 mbsf) and are composed primarily of clays and silty clays with variable amounts (bearing- to rich-) of microscopic authigenic carbonates (fig. 5, table 1, and Site NGHP-01-21 Visual Core Descriptions). Clays bearing foraminifera, pyrite and plant debris were also encountered in Hole NGHP-01-21A as two thin intervals in Core

Table 1. Smear-slide data for Hole NGHP-01-21A.—Continued

Sample reference	Biogenic										Comments
Core, section, depth (cm, in section)	Fora-minifera	Carbonate shell fragments	Diatoms	Radio-larians	Silico-flagellates	Siliceous shell fragments	Sponge spicules	Fish remains	Other biogenic	Plant debris	
NGHP-01-21A											
4X-1,65	40	50									
4X-1,69	50	40									
8X-3,80	60	40									
9X-6,36	25	25									
12X-5,75	15	15									

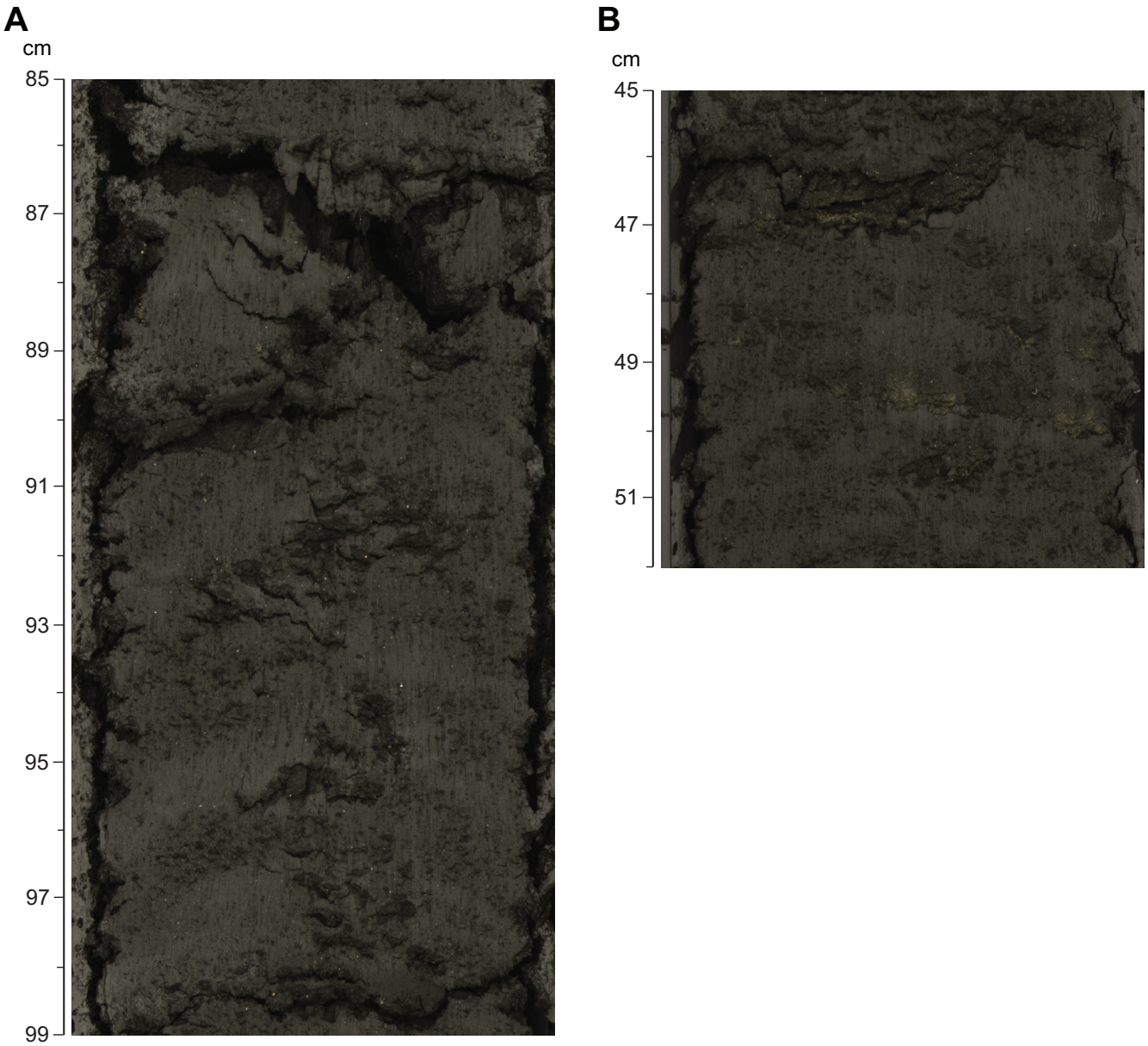

Figure 6. Examples of: A, silty clay zone in Section NGHP-01-21A-12X-5, 85–99 cm; and B, silt laminae in Section NGHP-01-21A-09X-5, 45–52 cm.

Table 2. Coarse-fraction data for Hole NGHP-01-21A.

Sample reference			Texture				Mineral									
Core, section, depth (cm, in section)	MBSF	Lithology	Sand	Silt	Clay	Quartz	Feldspar	Mica	Heavy minerals	Clay minerals	Volcanic glass	Glauconite	Framboidal pyrite	Iron sulfides	Rock framents	Authigenic carbonates
NGHP-01-21A																
1X-1,60	49.00	D		8	92	5				84				2		2
4X-2,10	61.12	D		15	85	5	1		1	71	1	trace		5		1
4X-2,52	61.54	D		10	90	7	1		trace	84	1	1		3		1
5X-1,10	64.60	D		15	85	5	1			73	3	1		3		8
6Y-1,65	69.65	D		15	85	5	trace		1	86	trace			2		5
6Y-1,69	69.69	M		20	80	4	trace		1	72	1		7	8		4
7E-1,40	70.40	D	3	10	87	8	trace	trace		66				trace	trace	15
8X-3,80	73.70	D		5	95	10				76						5
8X-4,43	74.83	M		3	97	10				79						3
9X-2,78	77.55	D	trace	15	85	10	trace	trace		76				3		8
9X-6,36	81.84	D		10	90	10	2	trace		78	3			3		
10Y-1,50	80.50	D		3	97	10				83						
12X-2,37	82.65	D	3	27	70	15	trace	trace		69				3		5
12X-6,60	86.96	D	3	35	60	30	trace	trace	2	54	3			5		3

Sample reference	Biogenic								Comments
Core, section, depth (cm, in section)	Foraminifera	Nannofossils	Carbonate shell fragments	Diatoms	Radiolarians	Silicoflagellates	Sponge spicules	Plant debris	
NGHP-01-21A—Continued									
1X-1,60	2	3						2	
4X-2,10	5	3						7	trace rutile
4X-2,52	trace	1						1	trace amphibole
5X-1,10	1	3					trace	2	
6Y-1,65	1			trace			trace	trace	trace chert or biogenic silica grains
6Y-1,69	trace	3		trace			trace	trace	from FeS rich zone
7E-1,40	3	3	trace	5			trace	trace	trace chert or biogenic silica grains
8X-3,80	3	2						4	
8X-4,43	3	2						3	
9X-2,78	trace	3		trace			trace	trace	trace chert or biogenic silica grains
9X-6,36	2	trace		trace				2	
10Y-1,50	2	1					trace	4	trace rutile
12X-2,37	trace	3		trace				5	trace chert or biogenic silica grains
12X-6,60	trace			trace				3	trace chert, trace reddish terrigenous grains

Note: M = minor lithology, D = dominant lithology

NGHP-01-21A-04X (fig. 5, table 1, and Site NGHP-01-21 Visual Core Descriptions). The dominance of pure and silty clays as well as the abundance of microscopic authigenic carbonate contrasts with the sediment sequences recovered above and below this depth interval at Sites NGHP-01-10 and NGHP-01-12 (fig. 5). At Sites NGHP-01-10 and NGHP-01-12, nannofossils are an important component in clays. Microscopic authigenic carbonates are below the limit of becoming an important lithologic component; instead, carbonates occur as micro-nodules and large nodules (fig. 5). If the sediment sequence recovered at Site NGHP-01-21 had been recovered at Site NGHP-01-10 or Site NGHP-01-12, it would have been justified to classify it as a separate lithologic subunit, which should be noted when considering the lithologic descriptions provided for holes with large zones of poor core recovery. Furthermore, the sediment package recovered at Site NGHP-01-21 suggests that possibly correlative packages of clays and silty clays were recovered at Sites NGHP-01-14, and NGHP-01-15 in the KG Basin (see "Lithostratigraphy" in "Site NGHP-01-14" and "Lithostratigraphy" in "Site NGHP-01-15").

Gas-Hydrate Occurrence

Evidence of gas hydrates was observed in four pressure cores from Hole NGHP-01-21A, one pressure core from Hole NGHP-01-21B, and four pressure cores from Hole NGHP-01-21C (see "Pressure Coring"). In the XCB cores in Hole NGHP-01-21A, moussey texture was observed in Cores NGHP-01-21A-01X, -04X, and -09X (figs. 5B and 8). Moussey textured and "salmon textured" cores were also observed in Pressure Core NGHP-01-21A-07E, which was split and described in the sedimentology lab. During NGHP Expedition 01, "salmon texture" was only observed in pressure cores at Holes NGHP-01-21, NGHP-01-10D, and NGHP-01-10B (See

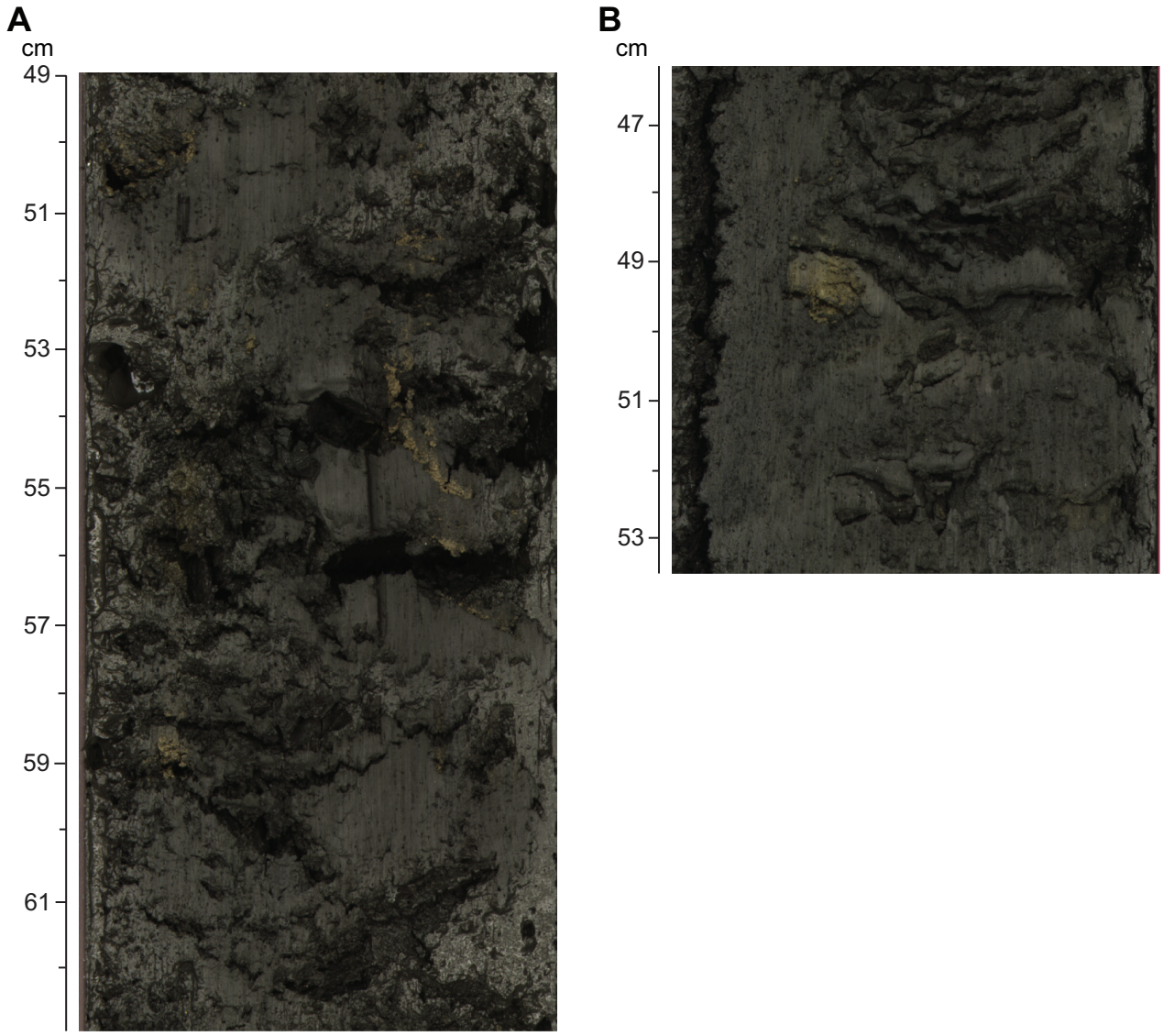

Figure 7. Examples of authigenic carbonate: A, enriched zone in Section NGHP-01-21A-01X-1, 49–62 cm; and B, micronodules in Section NGHP-01-21A-04X-2, 47–53 cm.

"Lithostratigraphy" in "Sites NGHP-01-10, 12, and 13") and thus may be a unique texture associated with gas hydrate dissociation or degassing of the pressure cores.

Because of the slightly coarser nature of the sediments recovered and described from XCB and from some pressures cores at Site NGHP-01-21, gas hydrates at this site may exist within the porosity of the silty clays or sand and silt beds and/or occur as fracture filling or disseminated gas hydrate (see "Pressure Coring"). These observations of the distribution of gas hydrate within the sediments, however, are biased by having limited pressure cores distributed throughout the holes and by poor XCB core recovery. Nevertheless, the split cores from Site NGHP-01-21 often showed moussey texture as described above (fig. 5 and Site NGHP-01-21 Visual Core Descriptions), which commonly results from the dissociation of gas hydrate and thus can be used to infer that gas hydrate was present throughout much of the gas hydrate occurrence zone at Site NGHP-01-21 (fig. 5B).

Inorganic Geochemistry

Site NGHP-01-21 was drilled in the KG Basin, approximately 10 m SE from Hole NGHP-01-10B and ~500 m NW from Site NGHP-01-12—both of these are sites with macroscopic gas-hydrate occurrences. Site NGHP-01-21 was washed to ~48 mbsf to target both the zone of high resistivity (see "Downhole Logging" in "Sites NGHP-01-10, 12, and 13") and the highest gas hydrate abundance recorded at Sites NGHP-01-10 and NGHP-01-12 (see "Inorganic Geochemistry" in "Sites NGHP-01-10, 12, and 13"). About 50 m were alternately drilled by XCB and pressure cored to a TD of ~90 mbsf, for a total of four XCB cores and six pressure cores. The main objectives were (1) to further map and characterize the subsurface distribution of gas hydrate in order to better understand the subsurface hydrology responsible for the accumulation of the gas hydrate deposits, (2) to conduct shipboard dissociation experiments at

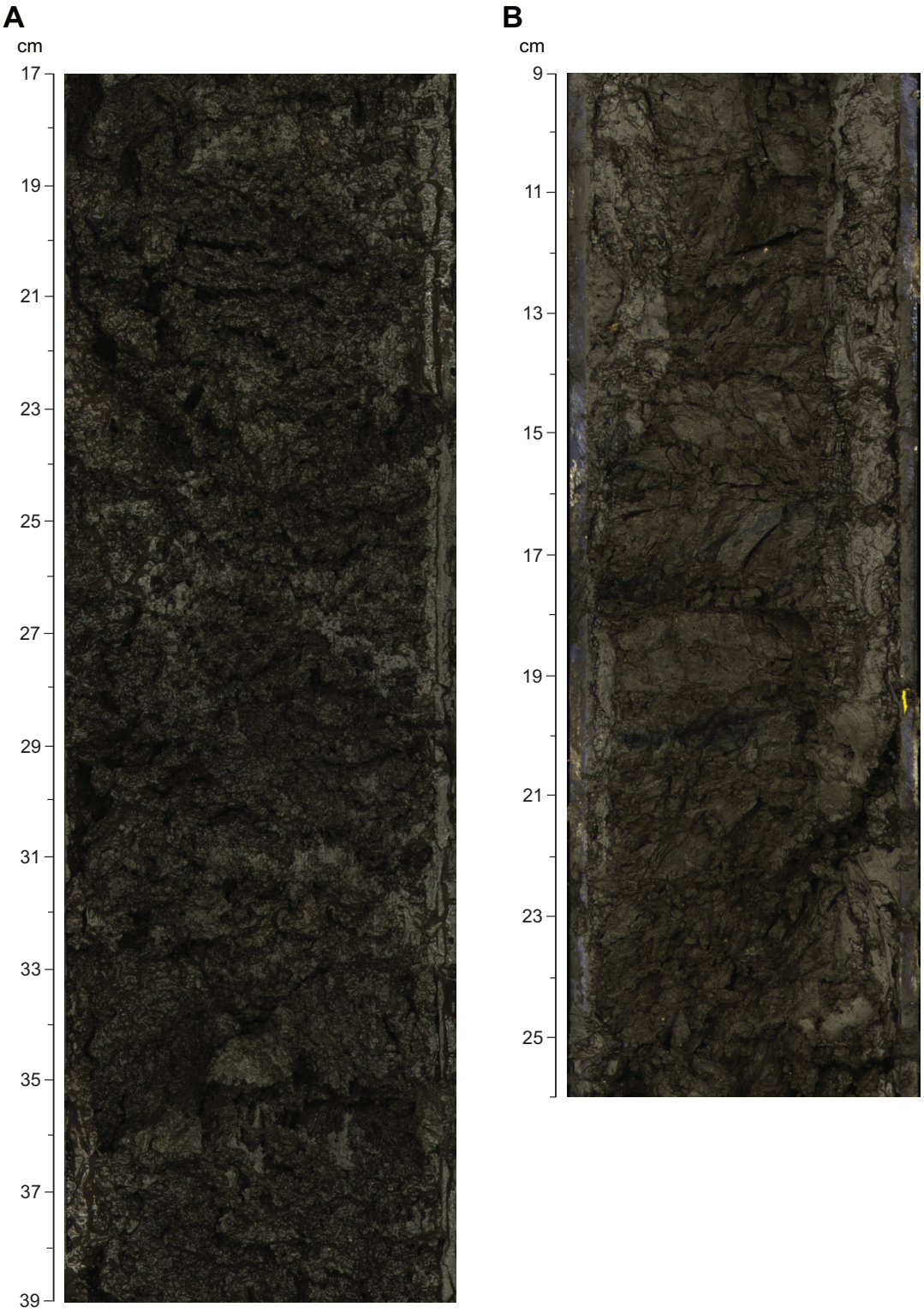

Figure 8. Examples of: A, moussey structure in Section NGHP-01-21A-04X-1; and B, salmon structure in Section NGHP-01-21A-07E-1.

Table 3. Interstitial-water data for Hole NGHP-01-21A.

["-", the value was not determined]

Sample name	Depth (mbsf)	Vol. (mL)	pH	Alk (mM)	Salinity	Titr Cl^- (mM)	Br^- (mM)	SO_4^{2-} (mM)	Comments
1X CC 0-25 HY	50.1	19.0	7.9	15.73	29.0	514	0.97	0.44	Two hydrate pieces decomposed in sediment. IR anomaly. Hydrate piece was very wet and difficult to clean from drill fluid.
1X CC 0-25 BK	50.1	18.0	8.1	13.58	31.0	557	1.04	1.44	Background was moussy and hard to clean.
1X CC 0-25 HY2	50.1	5.0	-	-	23.5	414	0.80	1.33	Left over slurry after cleaning the sample, labelled as "junk". Used to differentiate between hydrate and drill fluid. Subsamples only for in SO_4, Cl^- and isotopic analysis
4X-2 95-115	62.0	20.0	7.7	16.62	35.0	622	1.19	0.10	Sample showed lower cooling signal in catwalk.
4X-3 0-32 HY1	62.5	25.0	-	-	19.0	361	0.69	0.98	0–5cm: Large IR anomaly. Zone with nodules of hydrate. One piece of hydrate (~1.5cm × few mm) was still in squeezer.
4X-3 0-32 BK1	62.5	20.0	7.9	11.54	33.0	571	1.14	0.09	5–13.5cm: Moussy.
4X-3 0-32 HY2	62.5	20.0	-	-	25.0	431	0.84	1.82	13.5–17.5cm: This zone around area where hydrate vein occurred.
4X-3 0-32 BK2	62.5	23.0	-	-	32.0	568	1.11	0.13	17.5–30cm: Very moussy.
6Y-1 55-60 HY	69.6	7.0	-	-	29.0	519	1.05	0.07	Pressure core did not come under pressure, but contained IR anomaly. Core was split and working half was imaged by IR. Largest anomaly had small nodule. Sample was taken from section with max IR anomaly.
6Y-1 75-85 BK	69.8	13.0	-	-	34.0	600	1.21	0.04	Background sample did not look moussy.
7E 53-74	70.5	17.0	7.8	12.66	35.5	629	1.26	0.45	Pressure core with hydrate. ~70 liters of gas upon depressurisation. No X-ray scan available. Looked homogeneous upon opening.
8X-5 0-33 HY	75.9	19.0	7.9	9.95	20.5	220	0.81	0.66	0–7cm: Very wet. No difference in lithology throughout core 8X.
8X-5 0-33 BK1	75.9	11.0	-	-	33.0	576	1.22	0.07	7–15cm: No difference in lithology throughout core 8X.
8X-5 0-33 BK2	75.9	21.0	8.1	13.59	34.0	579	1.20	0.50	15–30cm: Rather Dry. No difference in lithology throughout core 8X.
9X-3 93-136 HY1	79.2	20.0	-	-	20.0	369	0.81	1.90	28–40cm: Scooped sediment with hydrate nodules from edge of core.
9X-3 93-136 HY2	79.2	16.0	-	-	34.5	593	1.27	0.50	28–40cm: Sediment taken from side of core without nodules. Rather dry.
9X-3 93-136 BK	79.2	15.0	8.1	13.77	39.5	663	1.34	0.07	6–15 cm.
10Y-1 72-82	80.7	15.0	-	-	35.0	463	1.00	0.04	Coldest part of pressure core. Did not come under pressure.
12X-4 0-35 HY	84.8	24.0	8.1	7.72	14.5	276	0.57	4.18	Core sample was sliced in half. Had many hydrate pieces in it.
12X-4 0-35 BK	84.8	16.0	7.9	16.42	30.5	547	1.11	0.74	Background sample contained no visible hydrate pieces.
Special Values									
12X-3 118-128 hydrate water		-	-	-	-	28	0.27	0.39	
12X-4 0-35 hydrate water	84.8	-	-	-	-	45	0.22	0.60	

Table 4. Interstitial-water data corrected for drill-water contamination based on sulfate concentration, for Hole NGHP-01-21A.

["-", the value was not determined]

Sample name	Depth (mbsf)	V Samp (mL)	pH	Alk (mM)	Salinity	Titr Cl^- (mM)	Br^- (mM)	Br^-/Cl^-	SO_4^{2-} (mM)
1X CC 0-25 HY	50.1	19.0	7.9	15.69	28.5	505	0.96	0.0019	0.00
1X CC 0-25 BK	50.1	18.0	8.1	15.69	30.5	548	0.96	0.0017	0.00
1X CC 0-25 HY2	50.1	5.0	-	-	23.0	405	0.79	0.0019	0.00
4X-2 95-115	62.0	20.0	7.7	16.62	35.0	622	1.19	0.0019	0.10
4X-3 0-32 HY1	62.5	25.0	-	-	17.8	342	0.66	0.0019	0.00
4X-3 0-32 BK1	62.5	20.0	7.9	11.54	33.0	571	1.14	0.0020	0.09
4X-3 0-32 HY2	62.5	20.0	-	-	22.8	396	0.79	0.0020	0.00
4X-3 0-32 BK2	62.5	23.0	-	-	31.8	565	1.11	0.0020	0.00
6Y-1 55-60 HY	69.6	7.0	-	-	29.0	519	1.05	0.0020	0.07
6Y-1 75-85 BK	69.8	13.0	-	-	34.0	600	1.21	0.0020	0.04
7E 53-74	70.5	17.0	7.8	12.82	35.5	630	1.27	0.0020	0.00
8X-5 0-33 HY	75.9	19.0	7.9	9.90	19.7	207	0.79	0.0038	0.00
8X-5 0-33 BK1	75.9	11.0	-	-	33.0	576	1.22	0.0021	0.07
8X-5 0-33 BK2	75.9	21.0	8.1	13.79	34.0	579	1.21	0.0021	0.00
9X-3 93-136 HY1	79.2	20.0	-	-	17.7	332	0.75	0.0023	0.00
9X-3 93-136 HY2	79.2	16.0	-	-	34.5	594	1.28	0.0022	0.00
9X-3 93-136 BK	79.2	15.0	8.1	13.77	39.5	663	1.34	0.0020	0.07
10Y-1 72-82	80.7	15.0	-	-	35.0	463	1.00	0.0022	0.04
12X-4 0-35 HY	84.8	24.0	8.1	7.38	9.4	195	0.45	0.0023	0.00
12X-4 0-35 BK	84.8	16.0	7.9	16.36	29.6	533	1.09	0.0020	0.00
Special values									
12X-3 118-128 hydrate water	-	-	-	-	-	20	0.26	0.0126	0.00
12X-4 0-35 hydrate water	84.8	-	-	-	-	33	0.20	0.0061	0.00

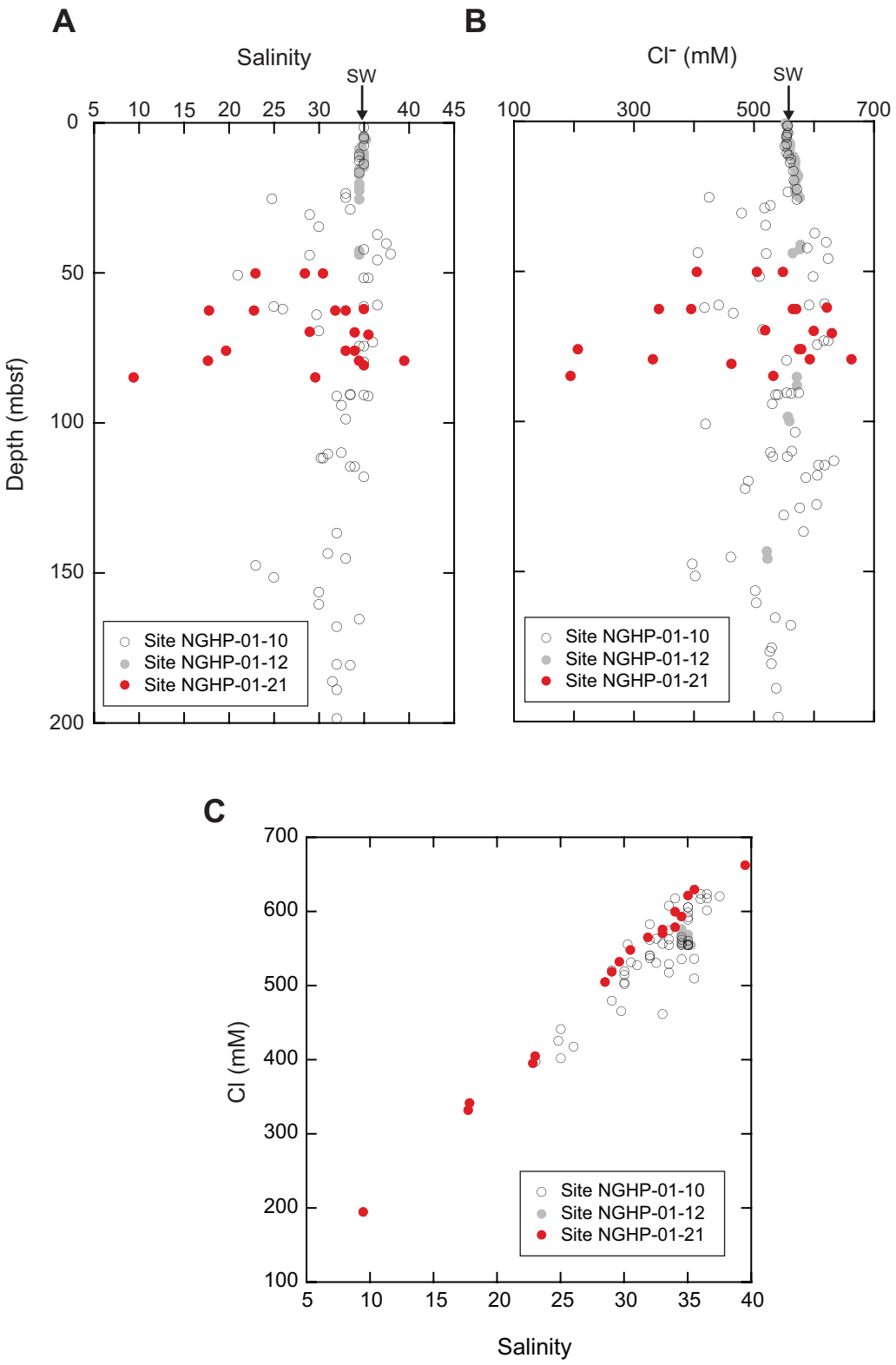

Figure 9. Concentration-depth profiles of: A, chloride; and B, salinity at Sites NGHP-01-10 (open circles), NGHP-01-12 (gray-filled circles) and NGHP-01-21 (red circles). C, Cross plot between dissolved chloride concentration and salinity, showing a generally good correspondence, suggests that at these sites these parameters are primarily influenced by dilution of the fluids by gas-hydrate dissociation. Deviations are likely due to the effect of diagenetic reactions that influence salinity but not chlorinity. Seawater value is designated as "sw" in A and B.

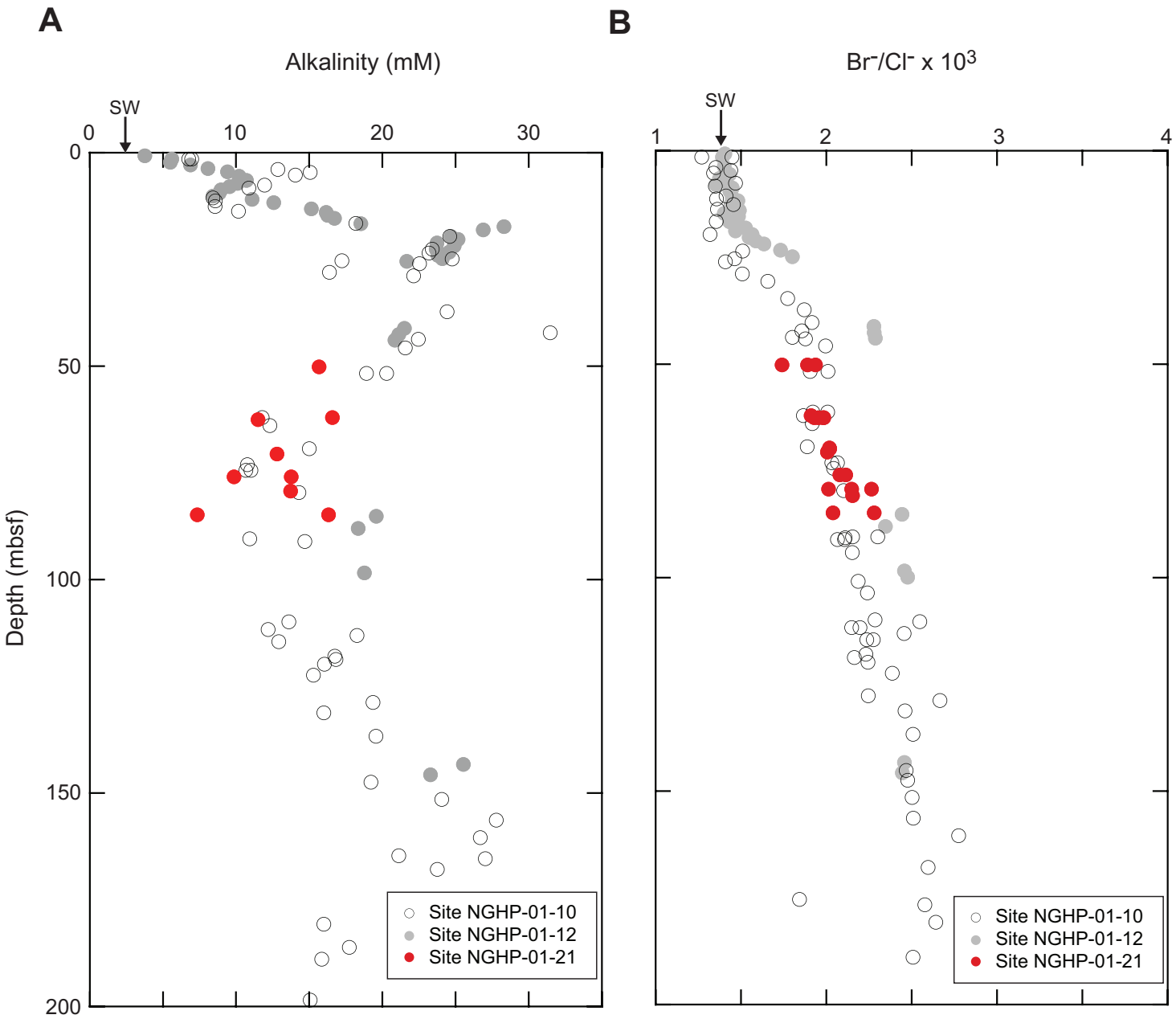

Figure 10. Concentration-depth profiles of A, alkalinity; B, sulfate; and C, Br^-/Cl^- at Sites NGHP-01-10 (open circles), NGHP-01-12 (gray filled circles), and NGHP-01-21 (red circles). The bromide data is shown as the ratio to chloride to reduce scatter related to gas-hydrate decomposition. Seawater values are designated as "sw" in A and B.

ambient pressure and temperature and to relate the observations to chemical and thermal imaging variations to better constrain the thermal imaging proxy for the abundance of gas hydrate, and (3) to recover and store gas hydrate samples in pressure cores and liquid nitrogen for specific post-cruise investigations. Interstitial water (IW) chemical composition data were obtained only in Hole NGHP-01-21A and are listed in tables 3 and 4 and illustrated in figures 9 and 10. Because this site was spot-cored, the data collected are presented in the context of the distributions observed at Sites NGHP-01-10 and NGHP-01-12.

A total of 10 whole round samples were collected for inorganic geochemical studies. These include four samples collected from Pressure Cores NGHP-01-21A-06Y, -07E and -10Y. The samples, which ranged in length from 25 to 43 cm, were specifically targeted to study the temperature history of gas hydrate dissociation (see "IR Imaging" in "Physical Properties") and to relate this to gas hydrate concentration estimated from dissolved chloride data and infrared (IR) temperature anomalies. Whole-round samples were selected based on IR imaging of the XCB cores on the catwalk. After rapidly slicing the core liner, each sample was immediately transferred to a recording station specially prepared for handling, continuous IR imaging, and photographing by digital video and still cameras, in order to relate visual and temperature changes as gas hydrate dissociates. After characterization by IR and photography, the sediments were sub-sampled for IW analyses to document the spatial gas-hydrate content based on chloride concentration. The sub-sampling was guided by the observed IR behavior. A total of 12 sub-samples from these whole rounds were squeezed and analyzed separately.

Interstitial Water Chloride and Salinity

As mentioned above, the main focus of sampling for IW analyses at Site NGHP-01-21 was to further understand the distribution and concentration of gas hydrate at this site, as well as to better constrain the thermal-imaging proxy for the abundance of gas hydrate. Thus, the strategies used for salinity and chloride sampling were driven by this specific goal. The data collected during this effort as well as data obtained from the adjacent Sites NGHP-01-10 and NGHP-01-12 (see "Inorganic Geochemistry" in "Sites NGHP-01-10, 12, and 13") are shown in figure 10. As noted at Sites NGHP-01-10 and NGHP-01-12, the zone of high variability in salinity and chloride occurs between 26 and 175 mbsf and reflects the distribution of gas hydrate. Consequently, this zone also reflects the distribution of IW freshening due to gas-hydrate dissociation. This zone coincides with the zone of RAB measured high resistivity (see "Downhole Logging" in "Sites NGHP-01-10, 12, and 13"). These resistivity logs further suggest that the highest concentration of gas hydrate occurs between ~45 and 87 mbsf, the depth interval targeted for coring and sampling at Site NGHP-01-21. The data in figure 9 show results both higher and lower than seawater salinity and chloride values. The minimum and maximum Cl^- values obtained at Site NGHP-01-21 are 195 and 663 mM (table 4), respectively, which correspond to ~35 percent and 120 percent of the modern seawater value. The sulfate concentrations in the IW samples were used to calculate the amount of drill-water contamination and correct chloride and salinity values. This was possible because all the samples recovered at Site NGHP-01-21 were from depths below the SMI that occurs at Site NGHP-01-10 at 19–24 mbsf (see "Inorganic Geochemistry" in "Sites NGHP-01-10, 12, and 13"). Thus, no sulfate was expected in the IW samples cored at Site NGHP-01-21.

The increase in Cl^- is due to *in situ* formation of gas hydrate, and that diffusion has not effectively transported all of the excess Cl^- from this interval, implying that gas hydrate actively formed *in situ* recently and may be forming at present.

Alkalinity and Bromide Concentrations.

Alkalinity and Br^- concentrations were also corrected for drill-water contamination. The corrected concentration values are listed in table 4 and shown in figure 10.

As shown in figure 10, the alkalinity data at Site NGHP-01-21 closely overlap the values obtained at Sites NGHP-01-10 and NGHP-01-12 (fig. 10A), indicating that organic matter diagenesis, including anaerobic methane oxidation and authigenic carbonate precipitation, occurs at similar rates at the three sites. A more detailed discussion of the alkalinity and sulfate-depth profiles is provided in "Inorganic Geochemistry" in "Sites NGHP-01-10, 12, and 13." The Br^-/Cl^- ratios (fig. 10B) obtained at Site NGHP-01-21 also overlap with the data obtained from Sites NGHP-01-10 and NGHP-01-12. The very similar ratios indicate that the same type of organic matter is responsible for the depth profiles seen in figure 10.

Macroscopic Hydrate Samples

Small pieces of massive hydrate were dissociated in syringes for gas analyses. The residual water was filtered to remove the sediment adhered to the gas-hydrate pieces, and was sub-sampled for shore-based analyses. Additional gas-hydrate pieces were dissociated in clean glass beakers, filtered, and sub-sampled for shore-based analyses of particularly the O and H isotopes of the gas-hydrate-framework water. Two samples were analyzed shipboard for sulfate, Cl^-, and Br^-—the data are included in tables 3 and 4. The sulfate data indicate contamination from drill-water, and the Cl^- and Br^- data indicate the amount of *in situ* seawater contamination. These data will be used to correct the isotope values.

Organic Geochemistry

The shipboard organic geochemistry program at Site NGHP-01-21 (GDGH-03-1B), an experimental step-out 10 m from Holes NGHP-01-10B and nearby Site NGHP-01-12, included analyses of the composition of volatile hydrocarbons including methane, ethane, and propane (C_1–C_3) and fixed natural gases (that is, O_2,

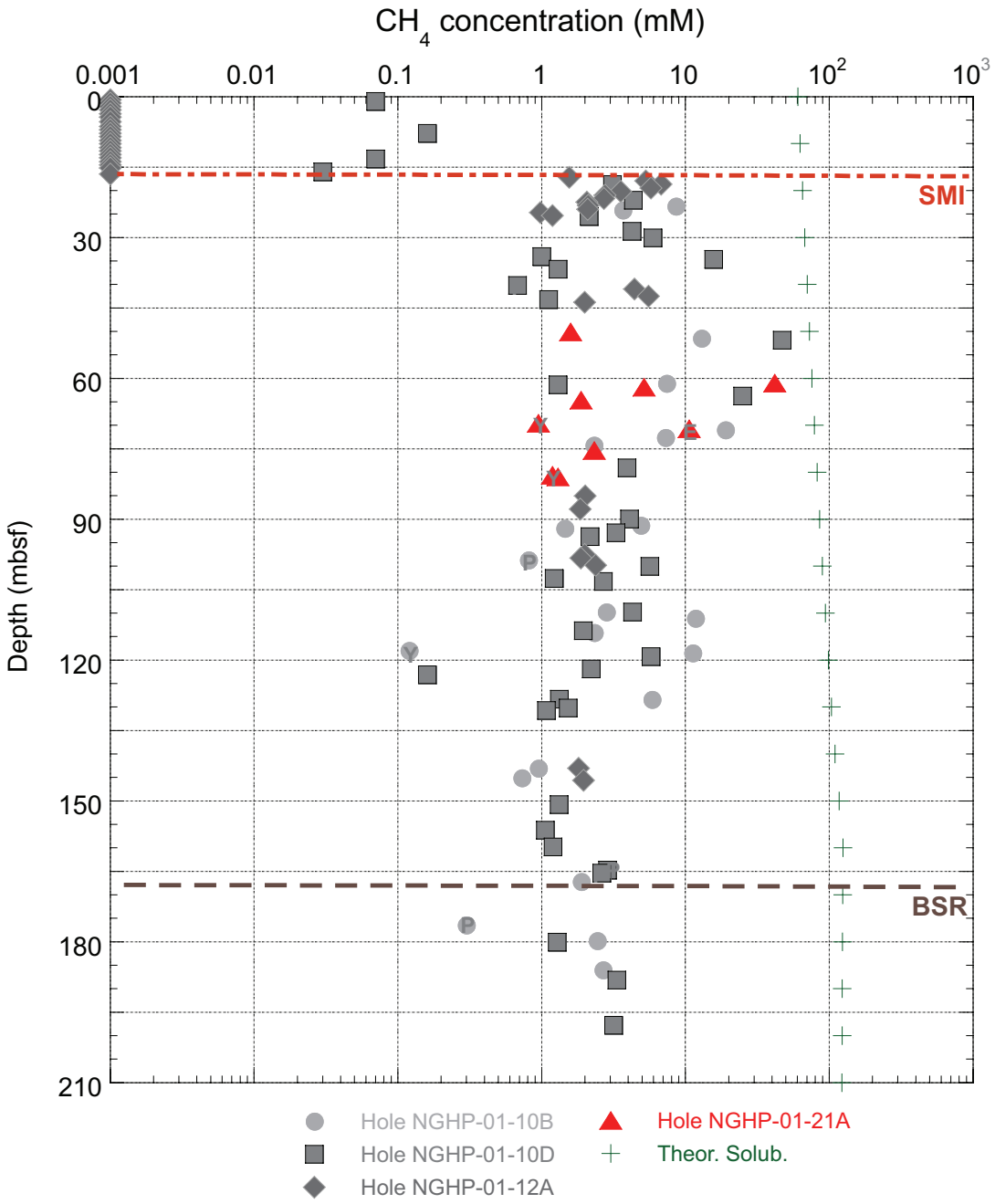

Figure 11. Plot of headspace methane gas concentration (mM) with depth for Site NGHP-01-21, Hole A (red triangles). Included in grayscale are the results of methane analyses performed at Sites NGHP-01-10 and NGHP-01-12 for reference. Notice the close association among gas chemistry results for these sites. Values less than 0.003 mM are below instrument detection limits, but plotted for reference. Text inside a symbol denotes special coring tool (E, HRC; P, PCS; Y, FPC). Theoretical solubility of methane calculated using the methods of Duan and others (1992) and Xu (2002, 2004).

Table 5. Headspace, void, and Pressure Core Sampler gas composition for Site NGHP-01-21. Pressure core samples annotated with sequential "+" refer to time intervals with +1 sampled first and +12 sampled last.

Sample reference	Interval (cm)	Sed wt. (g)	Sample depth (mbsf)	Time	CO_2 (ppm-v)	C_1	C_2	C_3	O_2	N_2+Ar	H_2S	C_1 (µL/L WS)	C_1 (mM PW)	CO_2 (µL/L WS)	CO_2 (mM PW)	C_1/CO_2	C_1/C_2
Headspace																	
21A-1X-CC	0	18.6	50.1	-	51,300	29,100	10	nd	140,100	749,300	nd	20,200	1.6	35,600	2.8	0.6	2,900
21A-4X2-0-5	0–5	8.6	61.0	-	19,600	212,200	50	nd	128,700	646,300	nd	565,000	41.8	52,100	3.9	10.8	4,200
21A-4X2-90-95	90–95	9.8	61.9	-	12,000	31,300	10	nd	144,800	792,200	nd	69,200	5.2	26,500	2.0	2.6	3,100
21A-5X1-90-96	14–19	14.0	64.6	-	6,200	19,500	nd	nd	154,900	787,000	nd	24,300	1.9	7,800	0.6	3.1	-
21A-6Y-28-33	28–33	9.7	69.6	-	19,900	5,600	nd	nd	62,300	875,800	nd	12,700	1.0	44,600	3.4	0.3	-
21A-7E-74-79	74–79	10.0	70.7	-	25,500	65,300	10	nd	138,100	766,800	nd	140,500	10.6	54,900	4.2	2.6	6,500
21A-8X4-96-101	96–101	10.5	75.4	-	22,000	15,200	nd	nd	149,900	786,100	nd	30,400	2.3	44,000	3.4	0.7	-
21A-9X5-105-110	105–110	10.5	81.0	-	4,800	8,400	nd	nd	166,300	789,700	nd	16,900	1.3	9,600	0.7	1.8	-
21A-10Y-67-72	67–72	16.9	80.7	-	109,800	16,900	nd	nd	114,100	747,100	nd	14,600	1.2	94,900	7.7	0.2	-
Void (free) gas																	
21A-9X3-30	30	-	78.5	-	1,700	995,400	210	nd	900	1,800	nd	-	-	-	-	590	4,700
21A-12X5-122	122	-	86.3	-	800	172,200	10	nd	175,,300	651,700	nd	-	-	-	-	220	17,200
Pressure core sampler																	
21A-7E-t1	-	-	70.0	1	200	787,200	200	nd	30,200	182,200	nd	-	-	-	-	3,940	3,900
21A-7E-t2	-	-	70.0	2	200	935,700	200	nd	11,900	52,100	nd	-	-	-	-	4,680	4,700
21A-7E-t3	-	-	70.0	3	500	367,000	40	nd	135,500	497,000	nd	-	-	-	-	730	9,200
21A-7E-t4	-	-	70.0	4	200	950,600	200	nd	9,600	39,400	nd	-	-	-	-	4,750	4,800
21A-7E-t5	-	-	70.0	5	700	2,100	100	nd	207,600	789,600	nd	-	-	-	-	3	21
21A-7E-t6	-	-	70.0	6	300	954,400	200	nd	9,000	36,100	nd	-	-	-	-	3,180	4,800
21A-7E-t7	-	-	70.0	7	200	959,200	200	nd	8,000	32,400	nd	-	-	-	-	4,800	4,800
21A-7E-t8	-	-	70.0	8	200	960,200	200	nd	7,400	32,000	nd	-	-	-	-	4,800	4,800
21A-7E-t9	-	-	70.0	9	200	957,700	200	nd	7,600	34,300	nd	-	-	-	-	4,790	4,800
21A-7E-t10	-	-	70.0	10	300	953,100	200	nd	7,800	38,700	nd	-	-	-	-	3,180	4,800
21A-7E-t11	-	-	70.0	11	300	926,800	200	nd	11,400	61,300	nd	-	-	-	-	3,090	4,600
21A-7E-t12	-	-	70.0	12	1,200	508,500	100	nd	103,400	386,800	nd	-	-	-	-	420	5,100

Notes: nd= not detected. WS = Wet sediment. PW = porewater. Approximate detection limits are about 15 ppmv for methane, 30 ppmv for ethane, 50 ppmv for propane, and 20 ppmv for hydrogen sulfide. Pressure core sampler degassing for times numbered 3, 5, 12 were likely contaminated with air to some degree during sampling/injection procedures

Table 6. List of microbiological samples taken for Site NGHP-01-21.

Sample reference Core, section	Sample code	Top (cm)	Bottom (cm)	Depth (mbsf)	Volume (cc)	Comments
NGHP-01-21A						
8X-2	MAF	25	35	72.7	374	
9X-2	MAF	127	137	78.04	374	
8X-2	MAG	35	45	72.8	374	
9X-2	MAG	137	147	78.14	374	
8X-2	MAR	15	25	72.6	374	
9X-2	MAR	117	127	77.94	374	
9X-5	MBF	120	130	81.18	374	
9X-5	MBG	130	140	81.28	374	
9X-5	MBR	110	120	81.08	374	

CO_2, and N_2+Ar) from headspace, void gas, and PCS degassing experiments. Results are similar to those described in more detail in "Organic Geochemistry" in "Sites NGHP-01-10, 12, and 13." Headspace gas analyses were performed on nine samples from NGHP-01-21A ranging in depth from 50.1 to 80.7 mbsf. Free gas or void gas samples were collected from two different void spaces ranging in depth from 78.5 to 86.3 mbsf. Gas was analyzed from one PCS degassing experiment in NGHP-01-21A (see "Pressure Coring" for details). The gas chemistry and concentration results showed similar trends to those observed at Sites NGHP-01-10 and NGHP-01-12 (fig. 11 and table 5; see "Sites NGHP-01-10,12, and 13").

In general, these analyses indicate that methane is the predominant hydrocarbon gas found in the cores at Site NGHP-01-21. However, ethane was present at low levels (<50 ppmv) in headspace below 50 mbsf and in moderate concentrations (<210 ppmv) in void and PCS gas samples collected below 70 mbsf. No propane (C_{3+})or higher molecular weight hydrocarbons were detected in gas samples. The headspace samples in the interval of 50–81 mbsf typify the results found at Sites NGHP-01-10 and NGHP-01-12 (fig. 11), as do other gas chemistry results at Site NGHP-01-21. For a complete downhole suite of results applicable to Site NGHP-01-21 (as indicated in fig. 11), please refer to the "Results" chapter for Sites NGHP-01-10 and NGHP-01-12.

Microbiology

Hole NGHP-01-21A

Analysis of all microbiological samples will be shore-based. Nine samples were collected for detailed microbiological studies under the following sample codes: MAF, MAG, MAR, MBF, MBG, and MBR (table 6).

Hole NGHP-01-21B

No microbiological samples were collected for this hole.

Hole NGHP-01-21C

No microbiological samples were collected for this hole.

Physical Properties

Introduction

Five whole-round XCB cores recovered at NGHP Expedition 01, Site 21 were imaged using the IR camera-track system on the catwalk to determine the location of temperature anomalies on the surface of core liners and to enable sections potentially containing gas hydrate to be quickly removed, preserved, and studied. After IR track imaging was finished, two additional types of experiments were performed on some core sections. One involved IR imaging and subsampling exposed sediment cores containing gas hydrate and the other alternated between IR imaging and scanning using the MSCL until all remnants of gas hydrate in the core were gone. The typical physical property program was attempted at Site NGHP-01-21; however, most of the recovered core sections were so badly disturbed that the program was quickly abandoned. See the "Physical Properties" section of the "Methods" chapter for more details.

The physical properties program at Site NGHP-01-21 focused on Hole NGHP-01-21A, which is drilled in the KG Basin (~36 km off the east coast of India) in about 1,037 m of water. Site NGHP-01-21 is located about 10 m SE of Hole NGHP-01-10B, a hole previously drilled during NGHP Expedition 01 that yielded significant amounts of gas hydrates. Hole NGHP-01-21A was washed down to about 48 mbsf, below which five XCB and six pressure cores were obtained. IR images indicated that significant amounts of gas-hydrate were present in many of the recovered cores.

IR Imaging

Environmental Conditions

The catwalk environment was monitored during the entire drilling operation at Hole NGHP-01-21A. Temperature on the catwalk averaged ~29 °C, ranging from 28.5 to 30.5 °C during the drilling operations, with relatively few significant temperature changes (fig. 12). Relative humidity ranged from 68 to 95 percent (fig. 12), which is consistent with a marine environmental setting of the northwestern Bay of Bengal, although there was a significant decrease in humidity during the latter part of the drilling. Adverse environmental conditions were not present during drilling operations at this site.

Near-surface seawater temperature was measured at this site using a temperature logger deployed over the port side at mid-ship. Seawater temperature was relatively constant at ~28.5 °C. However, data collected during the last third of coring shows considerable variation caused by heave pulling the temperature logger out of the water part of the time.

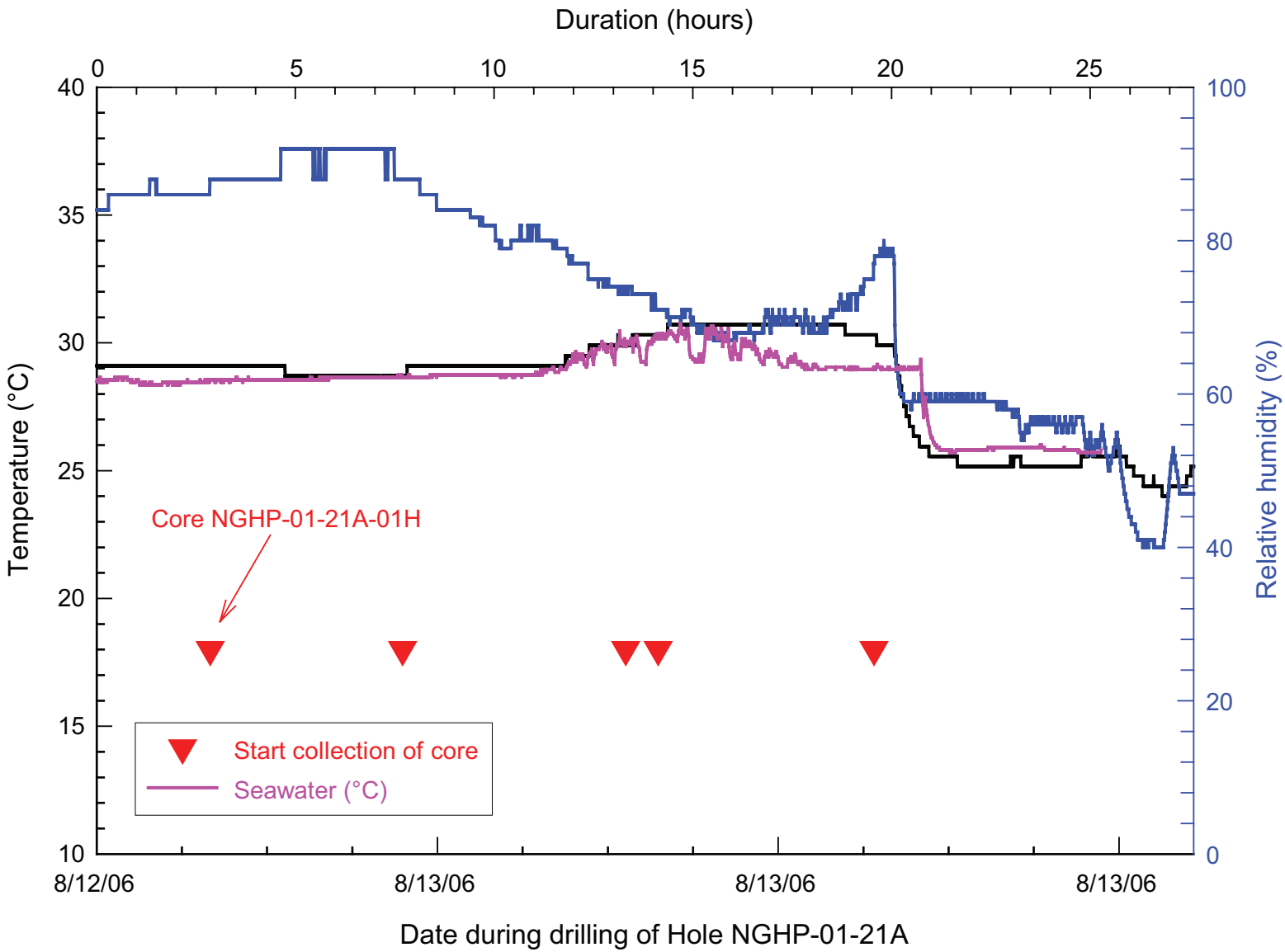

Figure 12. Catwalk temperature and humidity measurements as a function of time during drilling operations at Site NGHP-01-21.

IR Images

All five successful XCB cores from Hole NGHP-01-21A were systematically scanned upon arrival on the catwalk using the track-mounted IR camera described in the "Physical Properties" section of the "Methods" chapter. IR anomalies, commonly referred to as "cold spots," indicate gas-hydrate dissociation during core recovery, which subsequently provides guidance to catwalk sampling. Summary digital maps of the scans of all cores are available on the data DVD that accompanies this report, and listings of the image files are presented in table 7. Temperature arrays in text-formatted files were exported from the IR camera software and then concatenated for each core. The arrays were then further concatenated for all cores available in a given borehole. Downcore temperatures were averaged for each pixel row in the array, excluding pixels ~1 cm from the edge of the image and 2 cm along the midline of the image. The exclusion of these particular pixels minimized the effects caused by major thermal artifacts in the images. This processing enabled us to measure the average amplitude of the cold anomalies and to identify warm anomalies due to voids from the background-temperature field.

Coring at this site began at ~48 mbsf and was interspersed with pressure cores to harvest concentrated gas hydrate known to be present in this area from drilling and logging earlier in the expedition. IR track imaging at Site NGHP-01-21A consisted of five regular scans for a total scanned core length of ~40 m. The complete set of IR images collected for Hole NGHP-01-21A is presented in figure 13 along with the corresponding downcore temperatures. The core-liner surface temperature extracted from the IR images for Hole NGHP-01-21A ranged from a high of ~27 °C on void sections of the core liner throughout the hole to a low of ~15 °C in Core NGHP-01-21A-09X. Spikes at the end of cores approached 30 °C. Except for core NGHP-01-21A-01X, large parts of these cores were very cold and exhibited extensive expansion and significant loss of core material during retrieval and handling of the core barrel and liner, resulting in significant void space in the cores. As a result, IR scans are much longer than (in some cases more than double) the actual curated length of core. Figure 13 was therefore constructed by breaking out the downcore temperature plots and concatenated IR images of Core NGHP-01-21A-09X so that it does not overlap with the other cores. This approach shows the full distribution of both IR anomalies and voids in these cores. Selecting an appropriate background temperature is difficult for this core because of the extensive occurrence of gas hydrate. The red line at ~22 °C in figure 13 is the best estimate, indicating a change in temperature of up to 7 °C.

Section-End IR Images and Core-End-Temperature Readings

The typical section-end IR images and core-end-temperature readings were not taken on cores from Hole NGHP-01-21A because of the desire to rapidly preserve gas hydrate in cores or to initiate experiments on selected sections. However, core-end temperature probes were used to monitor core sections in some of the experiments described below.

Special Experiments on Selected Core Sections

Two types of experiments using IR imaging were conducted on selected core sections. First, sections were opened and still photographs, continuous video, and IR images were collected every 15 seconds as exposed gas hydrate dissociated. Once dissociation was nearly complete, the cores were taken to the chemistry lab for pore-water extraction and chemical analyses of sediments with and without gas hydrate (see "Inorganic Geochemistry"). The IR and digital video and still images have been analyzed post-cruise, and this analysis has focus on relating the temperature changes during gas-hydrate dissociation to the observed gas-hydrate occurrence and the pore-water chemistry, particularly the chlorinity values.

Second, selected sections were repeatedly scanned on the IR track and logged on the MSCL as gas hydrate dissociated within the liner. The purpose of these experiments is to relate the resistivity and density changes during gas-hydrate dissociation to the temperature change observed on the IR track. Typical cycle times for completing a set of both measurements was about 15 min. Temperature probes described in the "Physical Properties" section of the "Methods" chapter were also used to monitor section end temperatures during these experiments. IR scans for the experiments are listed in chronological order in table 7. The MSCL data are included in the MSCL database and can be linked to the IR data by section identifier and the information in table 7.

Determination of Thermal Emissivity of Marine Sediment

After the completion of IR imaging of cores from Hole NGHP-01-21A, a missed mudline core (Hole NGHP-01-3B 1H0-5) was retrieved from the hold where it had been stored at 4 °C. A window ~3 cm wide was cut out of the liner, exposing near-seafloor sediment. The section was instrumented with two temperature probes at each end and repeated IR scans were made as the sediment warmed to the ambient catwalk temperature at about 29 °C. One of the temperature probes was located just below the sediment surface. The outer layer of sediment was scraped away, exposing fresh sediment and the equilibrated temperature probe. The initial IR scan was performed immediately, including a scan of emissivity standards (black electrical tape and cardboard). Repeated scans were performed and a fifth temperature probe was introduced at the middle of the section just under the sediment surface. Data from this have been processed to estimate the thermal emissivity of marine sediment over the temperature range of ~10 °C to 29 °C (table 8). This information will add to a very limited sediment emissivity dataset and is critical to obtaining accurate temperature estimates from IR images of wet marine sediment.

Table 7. List of infrared images, including repeated scans, collected from Hole NGHP-01-21A.

Site:	NGHP-01-21			NGHP Expedition 01			
Hole:	A			Infrared Thermal Imaging Track			
Core	Imaging length (cm)	First run	Second run	Date (09/20)	Start time (20:48)	Temperature (start/end) (°C)	Comments
1X	430	x		8/12	22:40	29.1/29.1	10 to 30 °C range, visible gas hydrate in upper part of core originally
1Xa	135		x	8/12	22:55	29.1/29.1	10 to 30 °C range
1Xb	110		R	8/12	23:04	29.1/29.1	Start of repeat runs, IR and MSCL, repeat IR runs designated “R”
1Xc	110		R	8/12	23:17	29.1/29.1	
1Xd	110		R	8/12	23:32	29.1/29.1	
1Xe	110		R	8/12	23:46	29.1/29.1	
1Xf	110		R	8/12	23:59	29.1/29.1	
1Xg	110		R	8/13	0:15	29.1/29.1	
1Xh	110		R	8/13	0:32	29.1/29.1	Last scan of 1X, end of repeat runs
4X	890	x		8/13	3:11	28.7/28.7	Full core scan
4Xa	100		x	8/13	3:40	28.7/28.7	Section scan
8X	950	x		8/13	8:25	29.9/29.9	
8Xa	100		R	8/13	8:48	28.7/28.7	No image
8Xa1	100		R	8/13	8:49	29.1/29.1	No image
8Xa2	100		R	8/13	8:50	29.9/29.9	Good run
8Xb	100		R	8/13	9:02	29.9/29.9	
9X	940	x		8/13	9:11	30.3/30.3	
8Xc	100		R	8/13	9:24	30.3/30.3	1 more run on 8X
9Xa	130		R	8/13	9:34	30.3/30.3	Beginning interleaving of 9X and 8X
8Xd	100		R	8/13	9:36	30.3/30.3	
8Xe	100		R	8/13	9:45	30.3/30.3	
9Xb	130		R	8/13	9:47	30.3/30.3	
8Xf	100		R	8/13	9:52	30.7/30.7	
9Xc	130		R	8/13	10:02	30.7/30.7	
8Xg	100		R	8/13	10:03	30.7/30.7	
9Xd	130		R	8/13	10:17	30.7/30.7	
8Xh	100		R	8/13	10:18	30.7/30.7	
9Xe	130		R	8/13	10:31	30.7/30.7	
8Xi	100		R	8/13	10:32	30.7/30.7	
9Xf	130		R	8/13	10:43	30.7/30.7	No scan. No core
9Xg	130		R	8/13	10:57	30.7/30.7	
9Xh	130		R	8/13	11:11	30.7/30.7	
12X	950	X		8/13	14:15	30.7/30.7	
12Xa	120		R	8/13	14:35	30.3/30.3	Section 5, used E logger bottom, F logger top 9. See electronic files.
12Xb	120		R	8/13	14:40	30.3/30.3	
12Xc	120		R	8/13	14:47	30.3/30.3	
13X				8/13			No scan. No core (last core on deck)

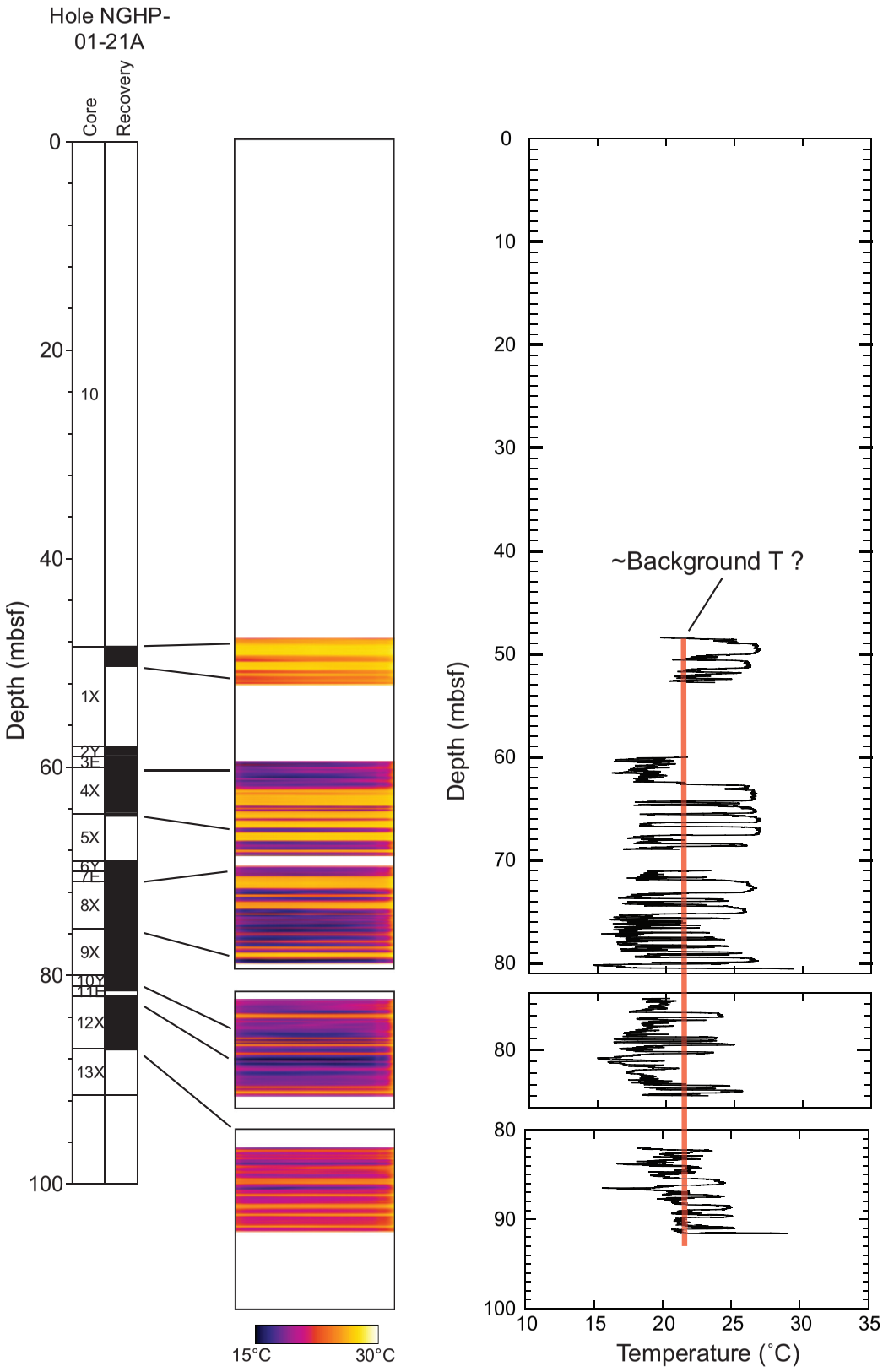

Figure 13. Infrared (IR) imaging and the derived downhole temperature profile for Hole NGHP-01-21A. Note that because of unequal core expansion during the recovery process, the length of core imaged using the IR track system was greater than the length of drilled core *in situ*. The diagram on the left side of the figure shows drilled core sections to scale. The right and middle diagrams show the expanded core sections imaged on the catwalk. [T, temperature]

Index Properties

The MSCL was used to measure physical properties from the XCB cores recovered at this site. However, the sediment was highly disturbed at many locations downcore, probably as a result of gas expansion caused by gas-hydrate dissociation. Bulk density values range between 1.4 and 1.6 g/cm^3 (fig. 14) and are more scattered than is typical for cores obtained during NGHP Expedition 01.

Electrical Resistivity

Resistivity values determined using the MSCL are in the typical range (varying by about 1 ohm-m) for sediment recovered during NGHP Expedition 01 (fig. 14). Lower MSCL values are more representative of less disturbed sediment as they are less impacted by the presence of voids caused by gas expansion.

P-Wave Velocity

All *P*-wave velocities (V_p) measured with the MSCL are very low and invalid. They reflect the disturbance caused to the sediment during the recovery process. Typically, V_p values are between 1.4 and 1.6 km/s, not below 0.9 km/s.

Magnetic Susceptibility

Magnetic susceptibility values are quite high and variable (fig. 14). These values are in agreement with holes drilled previously in the KG Basin during NGHP Expedition 01 and are due to the presence of primary and secondary terrigenous magnetic minerals (see "Lithostratigraphy"). It should be noted that sediment disturbance typically does not influence its magnetic susceptibility.

Pressure Coring

The main objectives of pressure coring during NGHP Expedition 01 were to quantify natural gas composition and concentration in sediments and to determine the nature and distribution of gas hydrate and free gas within the sediment matrix. Secondary objectives were to obtain measurements of physical properties on gas-hydrate-bearing sediments under *in situ* conditions, which can be used to help interpret regional seismic data, and to obtain samples under full pressure for shore-based studies. To achieve these objectives, we conducted depressurization experiments and captured resultant gas to calculate gas-hydrate quantity, made nondestructive measurements (X-ray imaging, *P*-wave velocity, gamma density) at *in situ* pressures and during depressurization to examine gas-hydrate habit within sediments.

Table 8. List of infrared (IR) data collected during IR scans to determine emissivity of wet marine sediment from Core NGHP-01-03B-1H-5.

IR track Run Designation	Comment
Emiss	First scan on core with sediment window cut out from 4 °C, starting ~17:15
Emiss1	Second and subsequent scans
Emiss2	
Emiss3	
Emiss4-1729	
Emiss5-1735	
Emiss6-1740	
Emiss7-1745	
Emiss8-1750	
Emiss9-1755	First scan with 2nd electrical tape
Emiss10-1800	Lots of condensation on liner (electrical tape wiped off just before scan
Emiss11-1807	F-4 temperature probe removed just before scan
Emiss12-1818	
Emiss13-1820	Upper part newly scraped cord from temperature probe got in the images
Emiss14-1821	No cord in view this time
Emiss15-1858	Divot removed at F-4 probe location just before scan (slightly cooler)
Emiss16-1921	Pulled F-4 probe and scraped deeply
Emiss17-1924	Next to last run
Emiss18-1925	Scraped end probe, should be a good match between probe T and IR T

Notes:

1. Used missed mudline section 3B 1H5 for this experiment
2. E-1, E-2 temperature probes top of section, inserted 8/13/06 17:15
3. E-3, E-4 temperature probes bottom of section inserted 8/13/06 17:15
4. F-4 probe insert in mid-top of core 8/13/06 18:07
5. Ambient T recorded for half the time with skate, RH and T device, typical 29.5 °C and 80% RH.

Hole NGHP-01-21A was offset 20 m to the NW with respect to Hole NGHP-01-10B, where massive gas hydrate had been collected earlier in the Expedition (see "Pressure Coring" in "Sites NGHP-01-10, 12, and 13"). The main objective of pressure coring at Site NGHP-01-21 was to recover pressure cores containing gas hydrate and transfer them into storage chambers for shore-based work.

Pressure-Core Operations and Measurements

Pressure-coring tools were deployed 12 times at Site NGHP-01-21 (table 9): six FPC cores (three in Hole NGHP-01-21A, one in Hole NGHP-01-21B, and two in Hole NGHP-01-21C) and six HRC cores (three in Hole NGHP-01-21A, one in Hole NGHP-01-21B, and two in Hole NGHP-01-21C). All HRC deployments used the new "Viking" auger bit (see "Pressure Coring" in "Site NGHP-01-17"). Figures 15 and 16 show the pressure and temperature history of the cores during deployment, coring, and recovery, and show the chilling of the

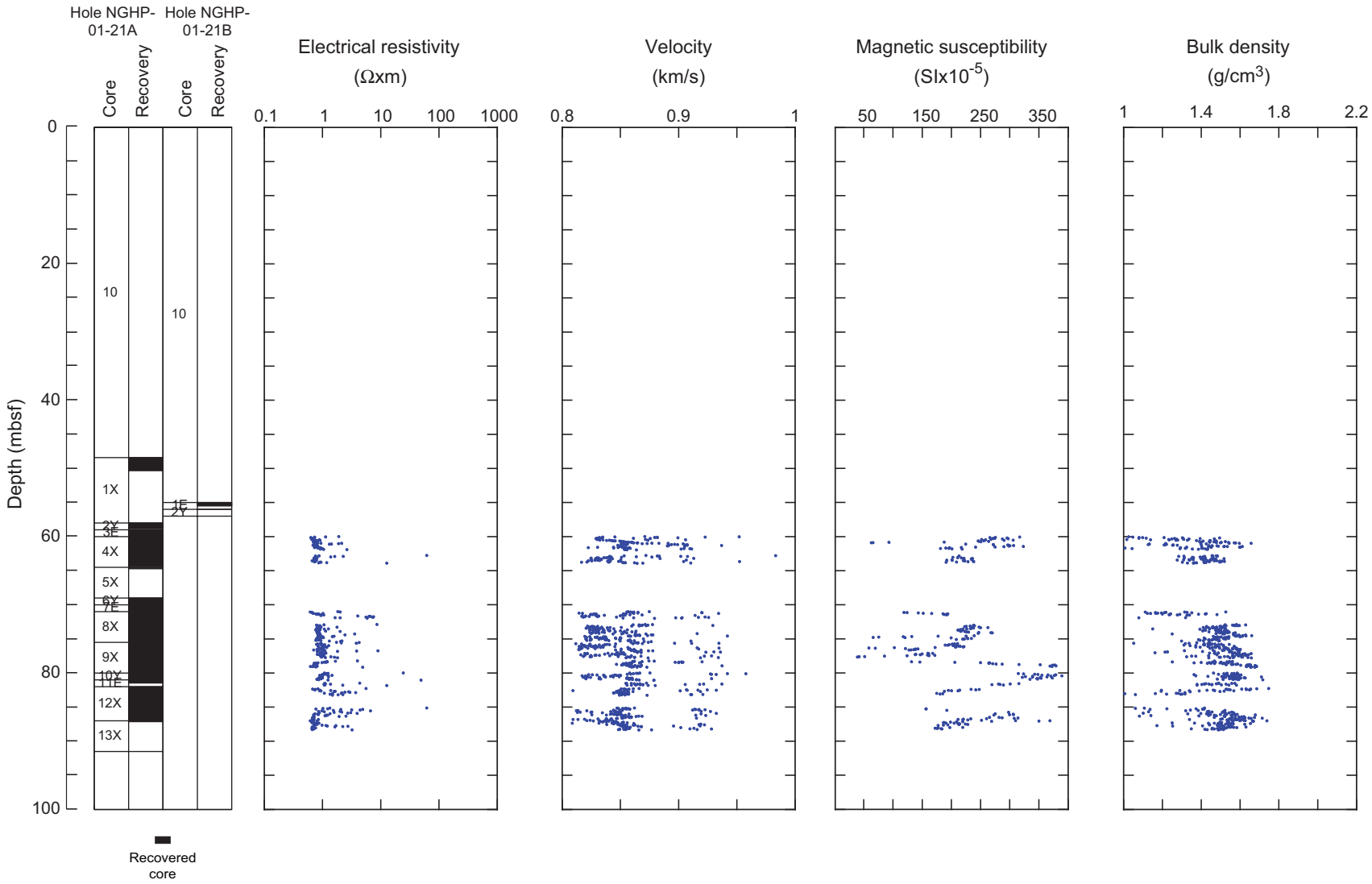

Figure 14. Profiles of core recovery, electrical resistivity, acoustic *P*-wave velocity, magnetic susceptibility, and bulk density for Site NGHP-01-21.

Table 9. Summary of pressure-coring operations at Site NGHP-01-21.

Core ID	Top of core (mbsf)	Length recovered (cm)*	Length curated (cm)*	Pressure at core depth (bar)	Pressure recovered (bar)		Comments
					logged**	gauge***	
NGHP-01-21A							
2Y	58.0	84	84	111	106	110	normal operation; stored in storage chamber
3E	59.0	108	108	111	100	105	used auger bit; stored in storage chamber
6Y	69.0	--	94	112	0	--	valve did not close
7E	70.0	109	109	112	100	103	stuck in transfer system; depressurized in autoclave
10Y	80.0	--	88	113	0	--	did not retract; data logger did not record
11E	81.0	47	47	113	96	100	used auger bit; stored in storage chamber
NGHP-01-21B							
1E	55.0	50	50	111	95	102	used auger bit; collapsed liner; sample into Parr vessel
2Y	56.0	--	0	111	0	--	did not fire
NGHP-01-21B							
1Y	55.0	85	85	111	124	120	could not transfer; put into Parr vessels
2E	56.5	110	110	111	104	105	used auger bit; stored in storage chamber
3Y	76.0	85	85	113	110	112	normal operation
4E	77.0	108	108	113	100	105	used auger bit; stored in storage chamber

Notes:
Water depth at Site NGHP-01-21 is 1049 m. Y=FPC, E=HRC.
*Length measured from X-ray and gamma density analysis, which may not match curated core length.
**Last pressure recorded before data logger disconnected from corer autoclave. Temperature 2–4 °C unless otherwise noted.
***Pressure measured when autoclave pressure transducer connected to external gauge. Pressure measured at 7 °C unless otherwise noted.

pressure-coring tools in the ice shuck. At this final site, after modifications had been made to both the HRC and FPC at previous sites, the pressure-coring tools had an overall success rate of 75 percent and recovered excellent, undisturbed cores.

Core NGHP-01-21A-02Y (58.0 mbsf) retrieved a full core (0.84 m) at full pressure (table 9). This core showed a brief increase in pressure as it warmed during handling on deck before being placed in the ice shuck. The core was transferred to the MSCL-P and X-ray images, gamma density and *P*-wave velocity measurements were collected (fig. 17A). X-ray images of the core showed massive gas hydrate in veins, both horizontal and vertical, along with light and dark bands that could indicate finely-distributed, grain-displacing gas hydrate. Evidence for gas hydrate was seen in the elevated and fluctuating *P*-wave velocities. Dark splotches on the X-ray image are likely to be carbonate nodules. Core NGHP-01-21A-02Y was transferred to storage chamber SC-2 (see "Singapore Pressure Core Studies" in the Appendix).

Core NGHP-01-21A-03E (59.0 mbsf) retrieved a full core (1.08 m) at full pressure (table 9). This core showed a brief increase in pressure as it warmed during handling on deck before it was placed in the ice shuck. The core was transferred to the MSCL-P and X-ray images, and gamma density and *P*-wave velocity measurements were collected (fig. 17B). X-ray images of the core showed a cluster of massive gas-hydrate veins crosscutting sedimentary bedding, with dense layers of hydrate interpreted as silts or sands. *P*-wave velocities were highest in the interval with the largest concentration of gas-hydrate veins (30–40 cm). Core NGHP-01-21A-03E was transferred to storage chamber SC-3 (see "Singapore Pressure Core Studies" in the Appendix).

Core NGHP-01-21A-07E (70.0 mbsf) retrieved a core (1.09 m) at pressure (table 10). The core became stuck in the transfer system before it could be examined in the MSCL-P, so no X-rays or other nondestructive measurements are available for this core. Core NGHP-01-21A-07E was depressurized in the corer autoclave/transfer system and released over 70 L of gas, which was the most gas released from a pressure core on NGHP Expedition 01. The methane released corresponded to 397.1 mL of methane hydrate or 31.5 percent methane hydrate as a percent of pore space. The pressure response vs. volume of gas released (fig. 18) and vs. time (fig. 19) did not show classic pressure plateaus and rebounds at 40–60 bar, though there was an apparent pressure plateau at the low pressure of 20 bar. The gas released was methane with approximately 200 ppm ethane, which is similar to what was found throughout the sediment column at Site NGHP-01-10 (see "Organic Geochemistry" in "Sites NGHP-01-10, 12, and 13"). There was no evidence of enhanced ethane.

Core NGHP-01-21A-11E (81.0 mbsf) retrieved a partial core (0.47 m) at pressure (table 9). This core showed a brief increase in pressure as it warmed during handling on deck before being placed in the ice shuck. The core was transferred to the MSCL-P, and X-ray images, gamma density, and *P*-wave velocity measurements were collected (fig. 17). X-ray images of the core showed that the bottom 20 cm of the core contained the largest concentration of gas hydrate collected in a pressure core on NGHP Expedition 01, with average core densities as low as 1.2 g/cc and *P*-wave velocities as high as 2,150 m/s. Core NGHP-01-21A-11E was transferred to Parr pressure vessels PV# 17 and 18 (0–25 cm and 25–47 cm, respectively). Massive gas hydrate was visible through the core liner during the transfer.

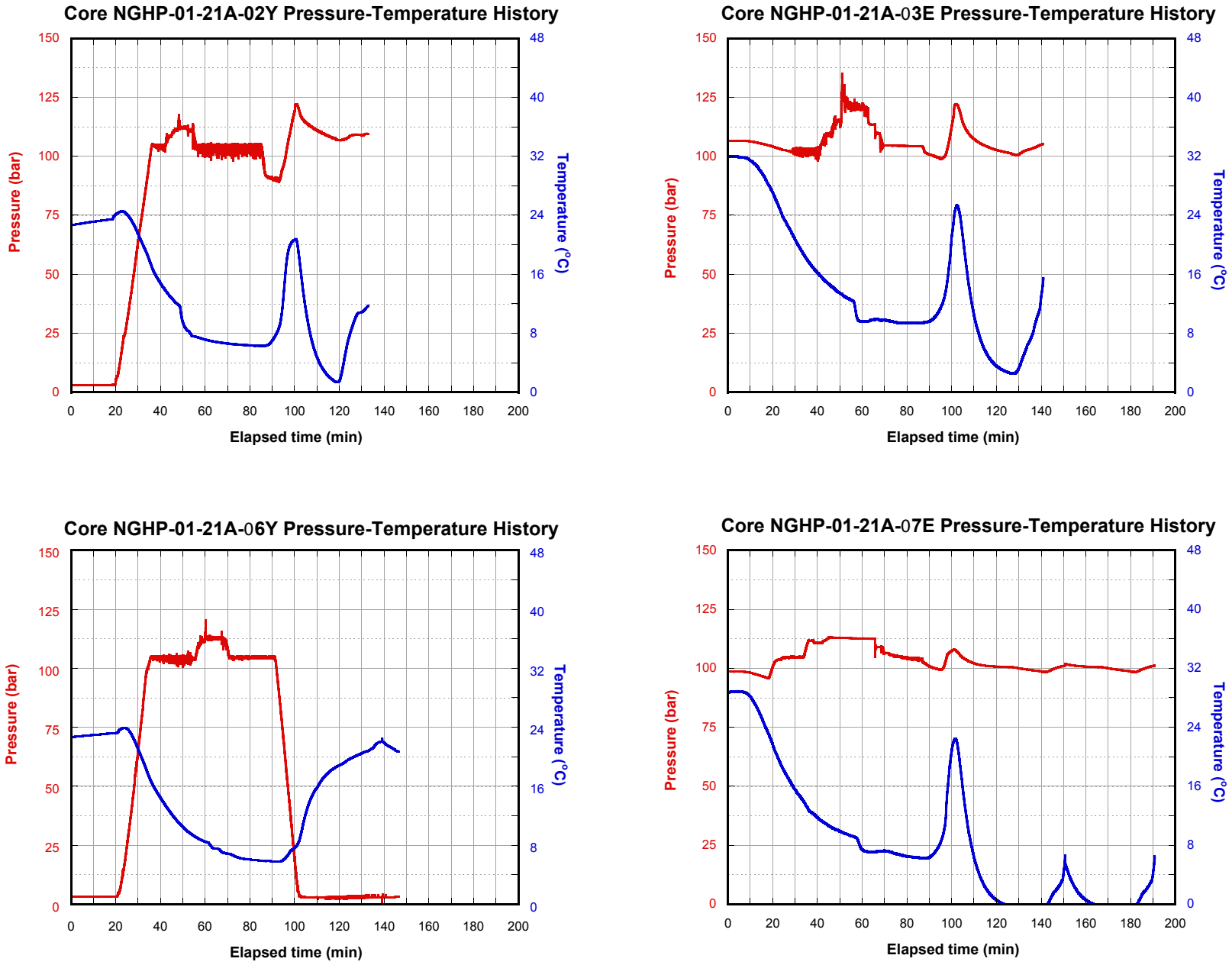

Figure 15. Temperature and pressure versus elapsed time for each pressure-corer deployment as recorded by the corer's internal data logger.

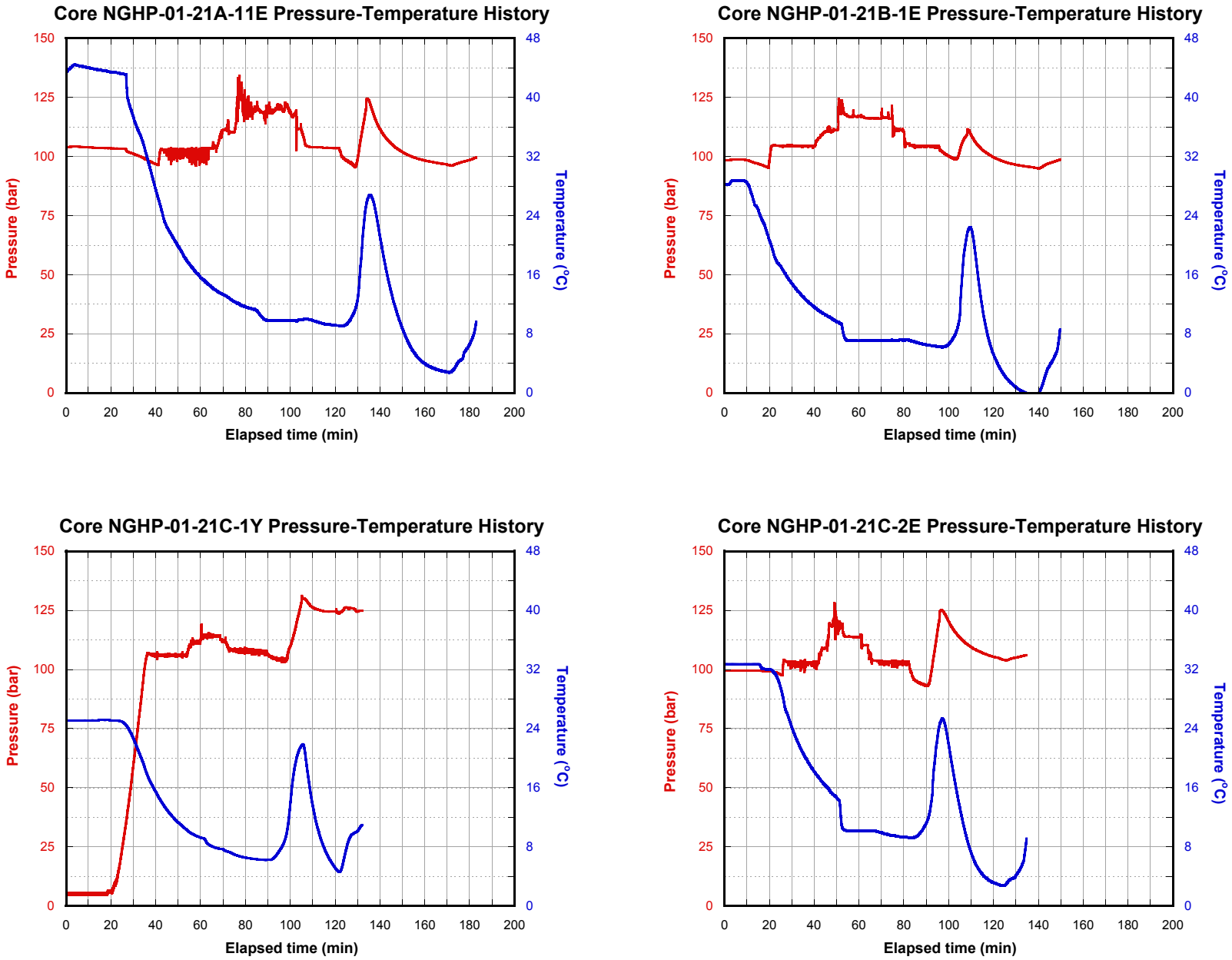

Figure 15. Temperature and pressure versus elapsed time for each pressure-corer deployment as recorded by the corer's internal data logger.—Continued

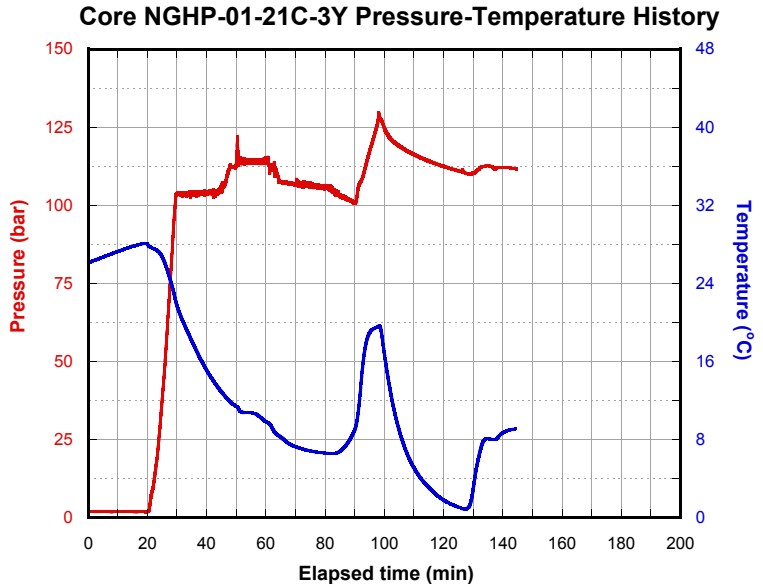

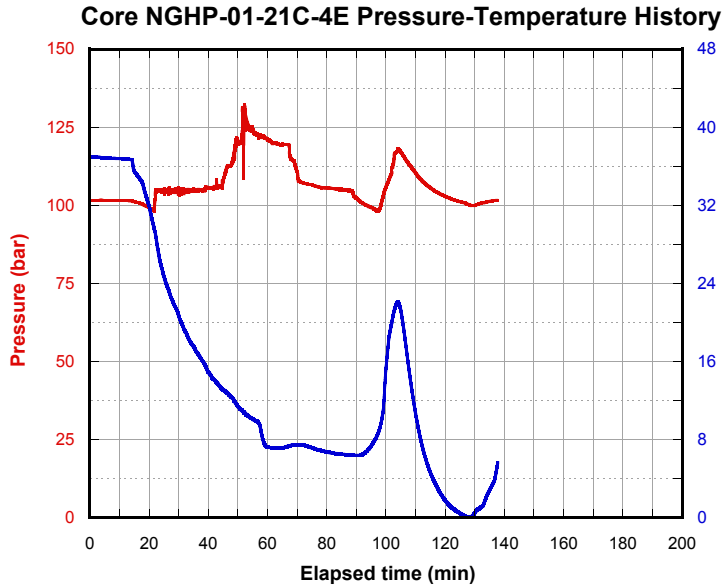

Figure 15. Temperature and pressure versus elapsed time for each pressure-corer deployment as recorded by the corer's internal data logger.—Continued

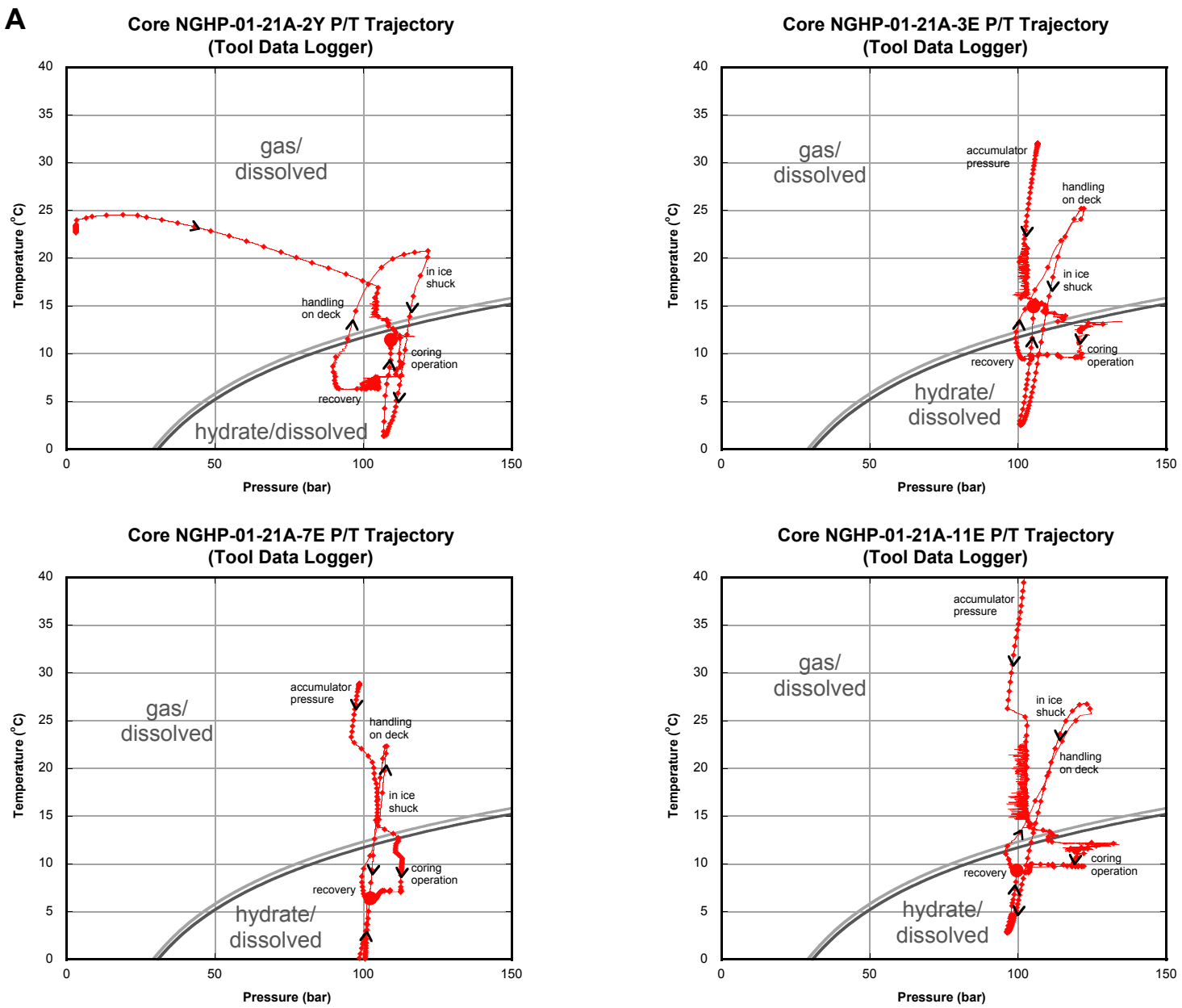

Figure 16. Temperature versus pressure for each successful pressure-corer deployment, showing trajectories relative to gas hydrate stability at 30 ppt and 35 ppt salinity, calculated from Xu (2002, 2004). A, Core NGHP-01-21A; B, Core NGHP-01-21B; C, Core NGHP-01-21C. Small dots are approximately every minute. Large dot is final temperature and pressure of autoclave prior to data logger removal. [ppt, parts per thousand]

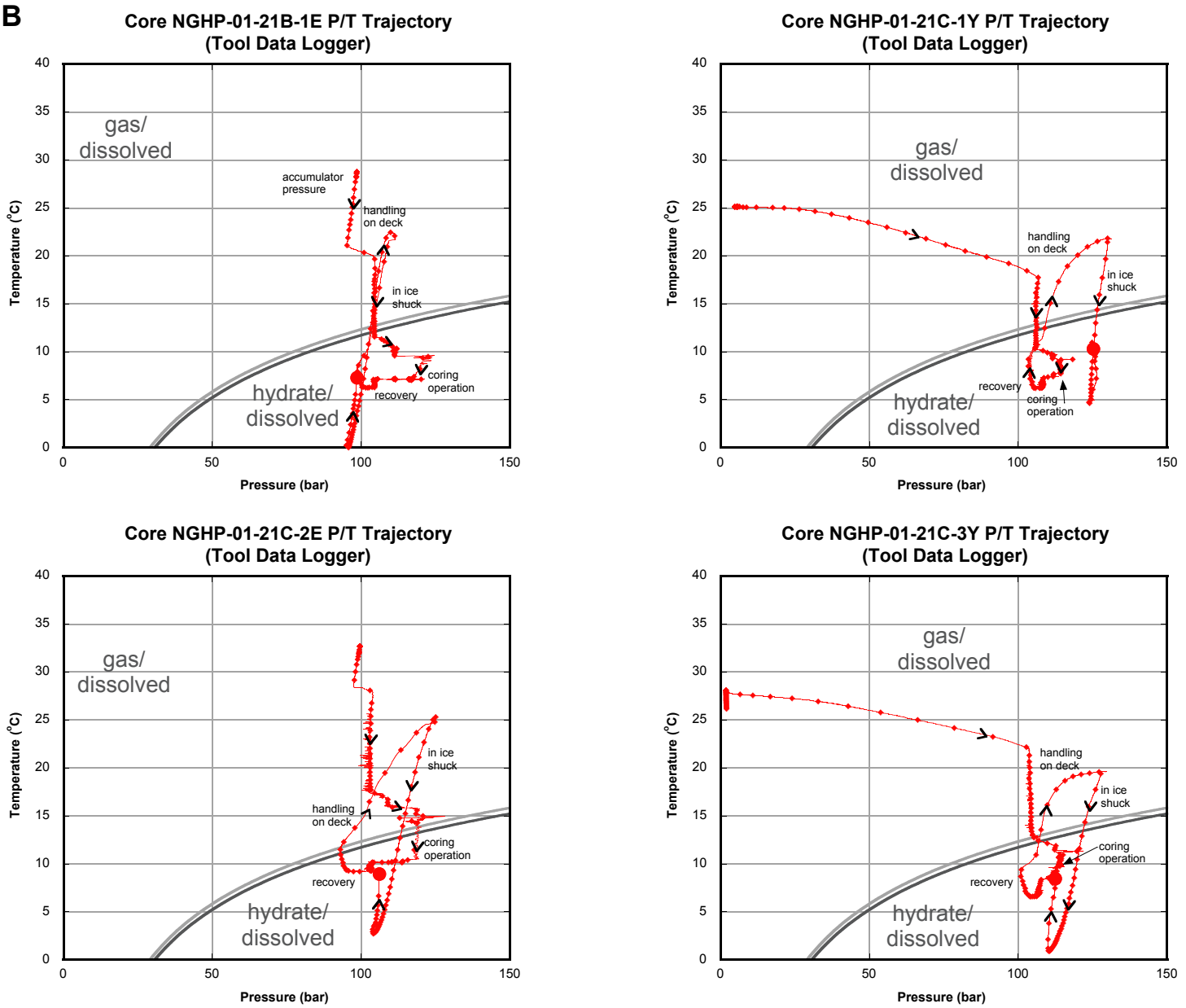

Figure 16. Temperature versus pressure for each successful pressure-corer deployment, showing trajectories relative to gas hydrate stability at 30 ppt and 35 ppt salinity, calculated from Xu (2002, 2004). A, Core NGHP-01-21A; B, Core NGHP-01-21B; C, Core NGHP-01-21C. Small dots are approximately every minute. Large dot is final temperature and pressure of autoclave prior to data logger removal. [ppt, parts per thousand]—Continued

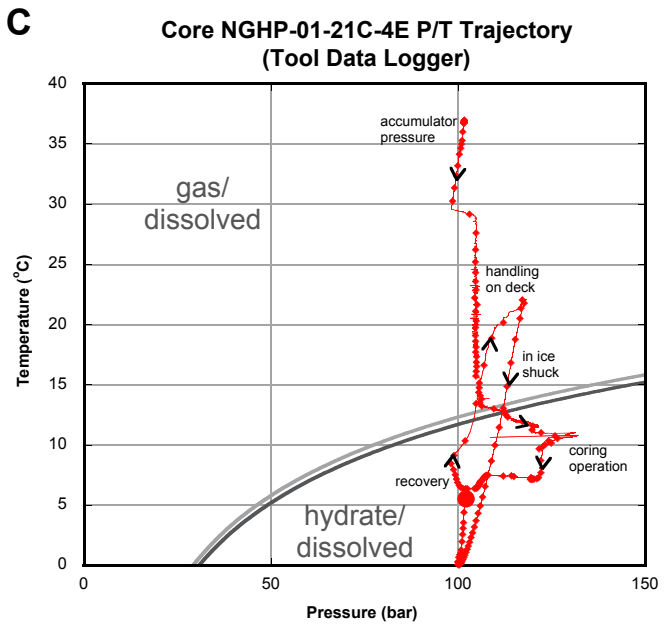

Figure 16. Temperature versus pressure for each successful pressure-corer deployment, showing trajectories relative to gas hydrate stability at 30 ppt and 35 ppt salinity, calculated from Xu (2002, 2004). A, Core NGHP-01-21A; B, Core NGHP-01-21B; C, Core NGHP-01-21C. Small dots are approximately every minute. Large dot is final temperature and pressure of autoclave prior to data logger removal. [ppt, parts per thousand]—Continued

Core NGHP-01-21B-01E (55.0 mbsf) retrieved a partial core (0.50 m) at pressure (table 9). The core was transferred to the MSCL-P, and X-ray images, gamma density, and *P*-wave velocity measurements were collected (fig. 17D). X-ray images of the core showed minor gas hydrate at the base of the core and that the top of the core liner had collapsed. This core was rapidly depressurized and the bottom 25 cm transferred quickly to Parr pressure vessel PV# 11.

Core NGHP-01-21C-01Y (55.0 mbsf) retrieved a full core (0.85 m) at full pressure (table 9). This core showed a brief increase in pressure as it warmed during handling on deck before being placed in the ice shuck. The core could not be transferred into the MSCL-P, so no X-ray images or other nondestructive measurements were collected on this core. Core NGHP-01-21C-01Y was rapidly depressurized, cut into four pieces, and each was transferred quickly to a Parr pressure vessel PV# 12, 14, 15,and 16 (0–20 cm, 20–41 cm, 41–61 cm and 61–85 cm, respectively). One-millimeter-thick gas-hydrate veins were observed in the sediment remaining in the core catcher.

Core NGHP-01-21C-02E (56.5 mbsf) retrieved a full core (1.10 m) at pressure (table 9). This core showed an increase in pressure as it warmed during handling on deck before being placed in the ice shuck. The core was transferred to the MSCL-P, and X-ray images, gamma density, and *P*-wave velocity measurements were collected (fig. 17). X-ray images of the core showed wispy gas-hydrate veins crosscutting horizontal sedimentary bedding, with dense silty or sandy layers. Core NGHP-01-21C-02E was transferred to storage chamber SC-4 (see "Singapore Pressure Core Studies" in the Appendix).

Core NGHP-01-21C-03Y (76.0 mbsf) retrieved a full core (0.85 m) at pressure (table 9). This core showed a brief increase in pressure as it warmed during handling on deck before being placed in the ice shuck. The core was transferred to the MSCL-P, and X-ray images, gamma density, and *P*-wave velocity measurements were collected (fig. 17F). X-ray images of the core showed wispy gas-hydrate veins crosscutting horizontal sedimentary bedding, with dense layers interpreted as silts or sands. Core NGHP-01-21C-03Y was transferred to Parr pressure vessels PV# 19 and 20 (0–25 cm and 50–75 cm, respectively) and liquid nitrogen (25–50 cm; hydrate sample HY140). As with Core NGHP-01-21C-01Y, 1-mm-thick gas-hydrate veins were observed in the sediment remaining in the core catcher.

Core NGHP-01-21C-04E (77.0 mbsf) retrieved a full core (1.08 m) at pressure (table 9). This core showed an increase in pressure as it warmed during handling on deck before being placed in the ice shuck. The core was transferred to the MSCL-P, and X-ray images, gamma density, and *P*-wave velocity measurements were collected (fig. 17G). X-ray images of the core showed wispy gas-hydrate veins crosscutting sedimentary bedding, with dense silty or sandy layers. Core NGHP-01-21C-04E was transferred to storage chamber SC-5 (see "Singapore Pressure Core Studies" in the Appendix).

Though Cores NGHP-01-21A-06Y and -10Y were not recovered under pressure, they still contained gas hydrate. These cores were used for special gas-hydrate dissociation experiments, as were the XCB cores at this site (see "Inorganic Geochemistry").

Gas-Hydrate Concentration, Nature, and Distribution from Pressure Coring

Methane concentration was only determined by depressurization for one of the cores at Site NGHP-01-21, Core NGHP-01-21A-07E. All other successful pressure cores were transferred into storage chambers for further work onshore. The methane concentration determined from Core NGHP-01-21A-07E, which was estimated to contain over 30 percent gas hydrate by pore volume, was comparable to other cores taken at Site NGHP-01-10 (fig. 20). A comparison between the MSCL-P data from the depressurized Core NGHP-01-10B-18Y (with 25 percent gas hydrate) and the stored cores from Site NGHP-01-21 suggests that the stored cores also contain 15–40 percent gas hydrate by pore volume.

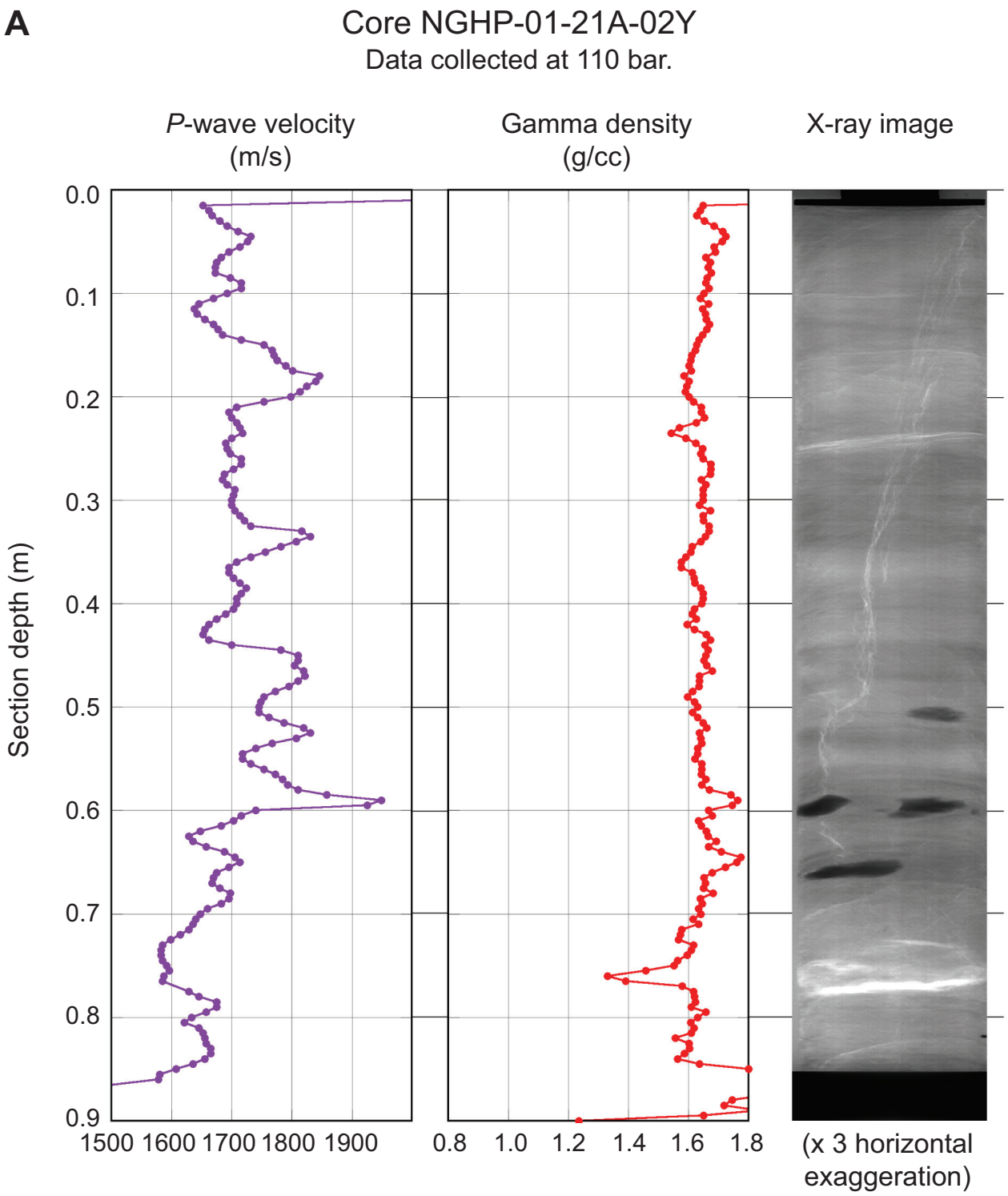

Figure 17. Data collected at near-*in situ* pressure and at 7 °C for successful pressure cores, including X-ray images, gamma density, and *P*-wave velocity. A, Core NGHP-01-21A-02Y; B, Core NGHP-01-21A-03E; C, Core NGHP-01-21A-11E; D, Core NGHP-01-21B-01E; E, Core NGHP-01-21V-02E; F, Core NGHP-01-21C-03Y; G, Core NGHP-01-21C-04E. X-ray images have been stretched 300 percent in the cross-core direction to show detail.

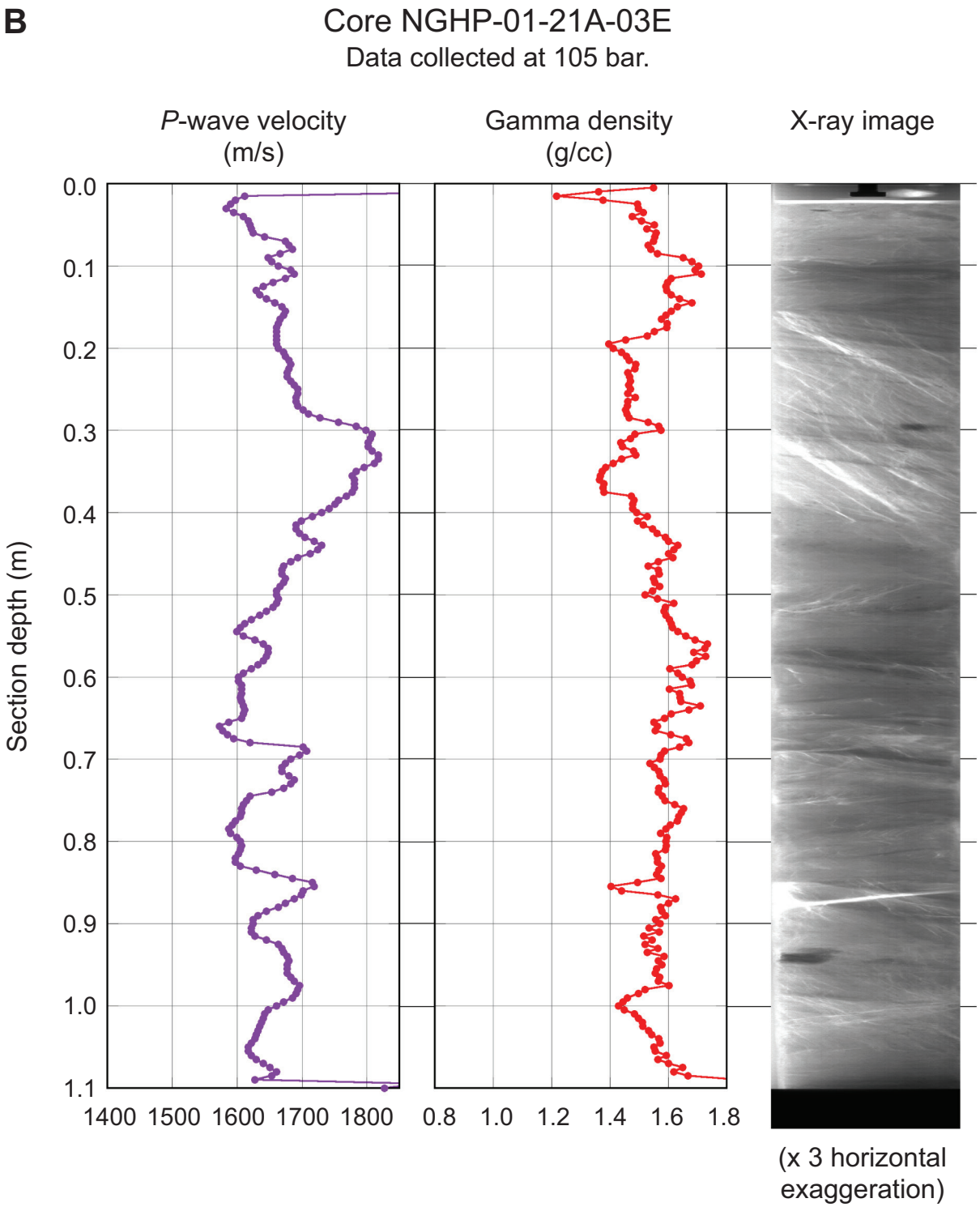

Figure 17. Data collected at near-*in situ* pressure and at 7 °C for successful pressure cores, including X-ray images, gamma density, and *P*-wave velocity. A, Core NGHP-01-21A-02Y; B, Core NGHP-01-21A-03E; C, Core NGHP-01-21A-11E; D, Core NGHP-01-21B-01E; E, Core NGHP-01-21V-02E; F, Core NGHP-01-21C-03Y; G, Core NGHP-01-21C-04E. X-ray images have been stretched 300 percent in the cross-core direction to show detail.—Continued

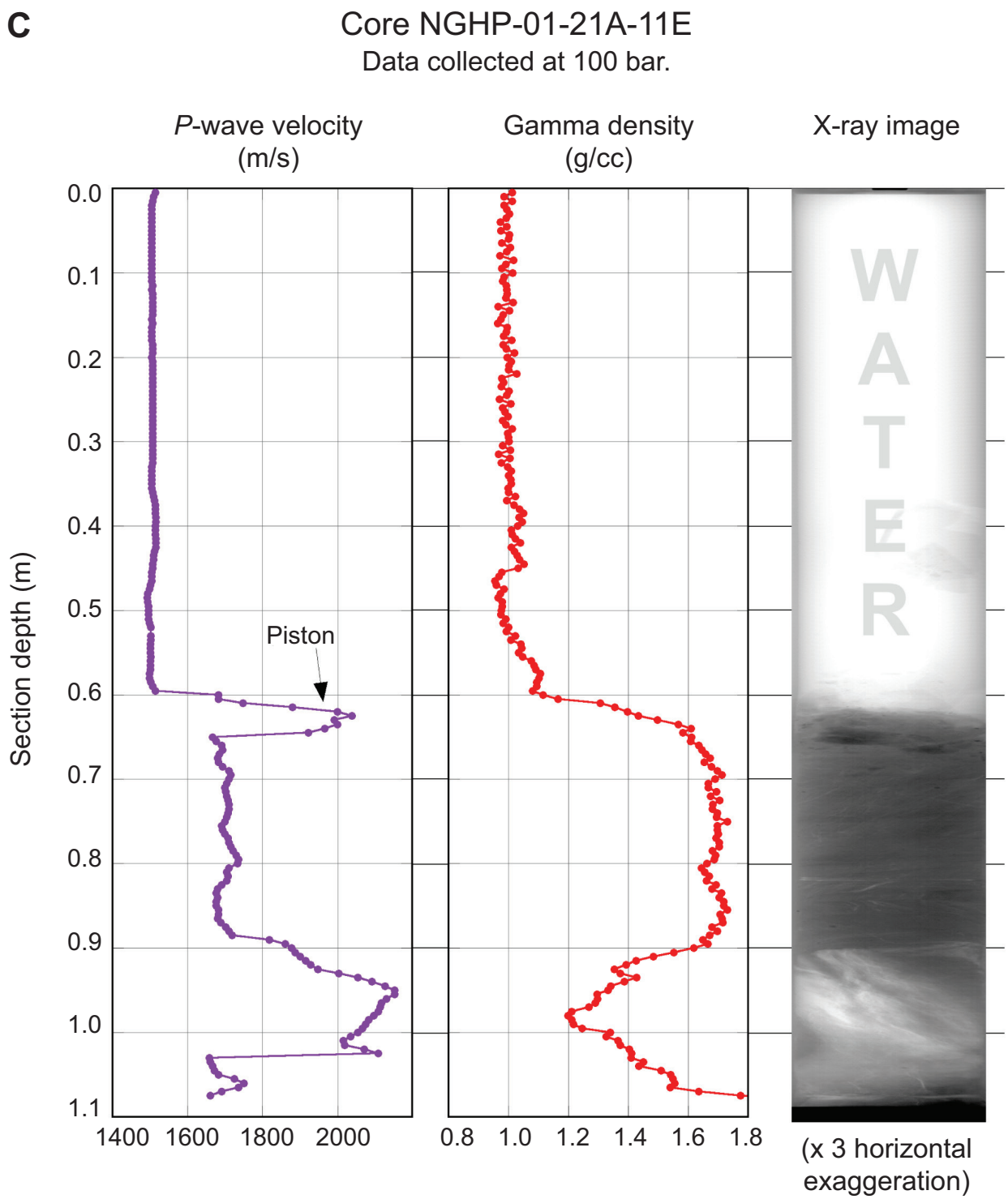

Figure 17. Data collected at near-*in situ* pressure and at 7 °C for successful pressure cores, including X-ray images, gamma density, and *P*-wave velocity. A, Core NGHP-01-21A-02Y; B, Core NGHP-01-21A-03E; C, Core NGHP-01-21A-11E; D, Core NGHP-01-21B-01E; E, Core NGHP-01-21V-02E; F, Core NGHP-01-21C-03Y; G, Core NGHP-01-21C-04E. X-ray images have been stretched 300 percent in the cross-core direction to show detail.—Continued

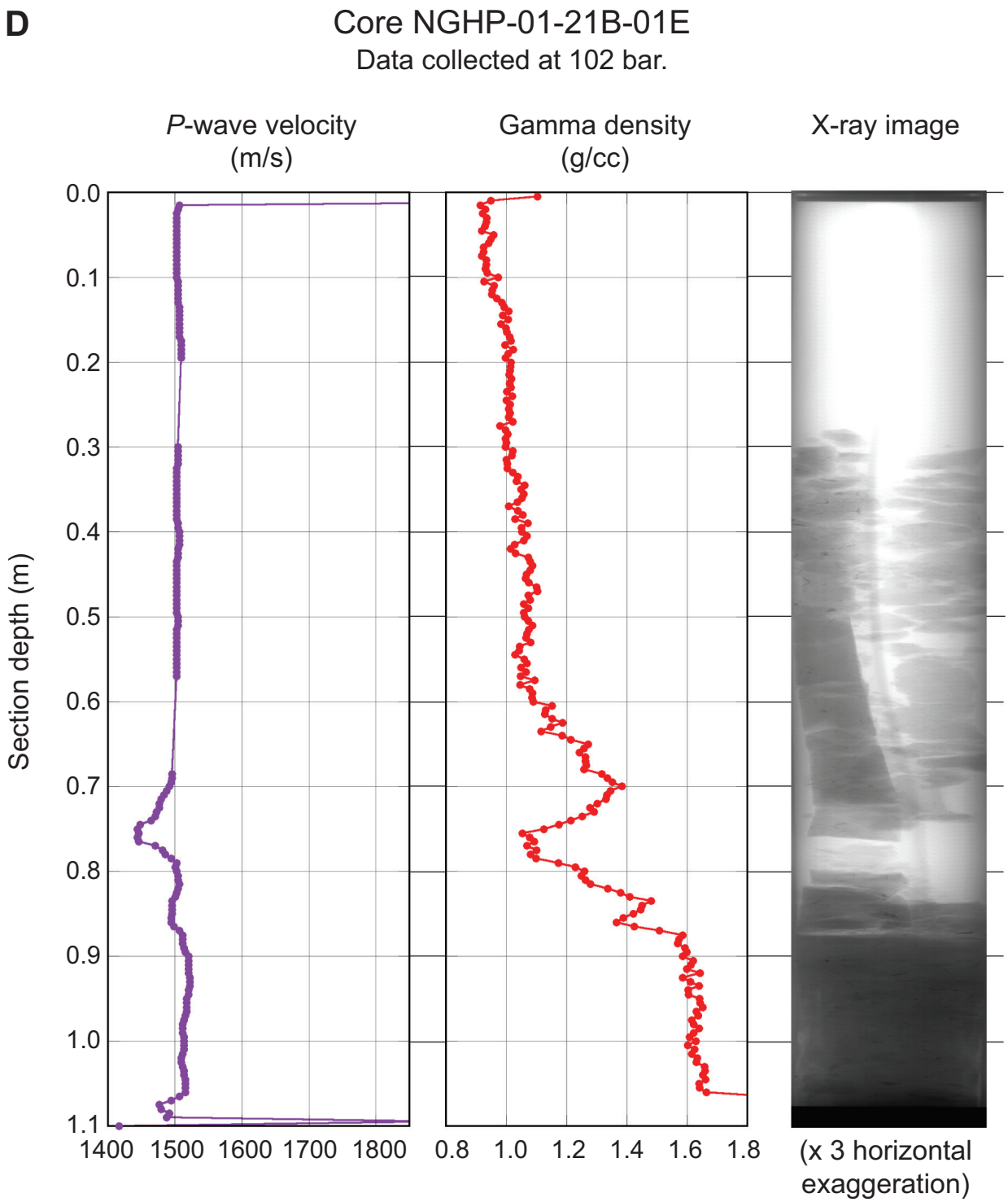

Figure 17. Data collected at near-*in situ* pressure and at 7 °C for successful pressure cores, including X-ray images, gamma density, and *P*-wave velocity. A, Core NGHP-01-21A-02Y; B, Core NGHP-01-21A-03E; C, Core NGHP-01-21A-11E; D, Core NGHP-01-21B-01E; E, Core NGHP-01-21V-02E; F, Core NGHP-01-21C-03Y; G, Core NGHP-01-21C-04E. X-ray images have been stretched 300 percent in the cross-core direction to show detail.—Continued

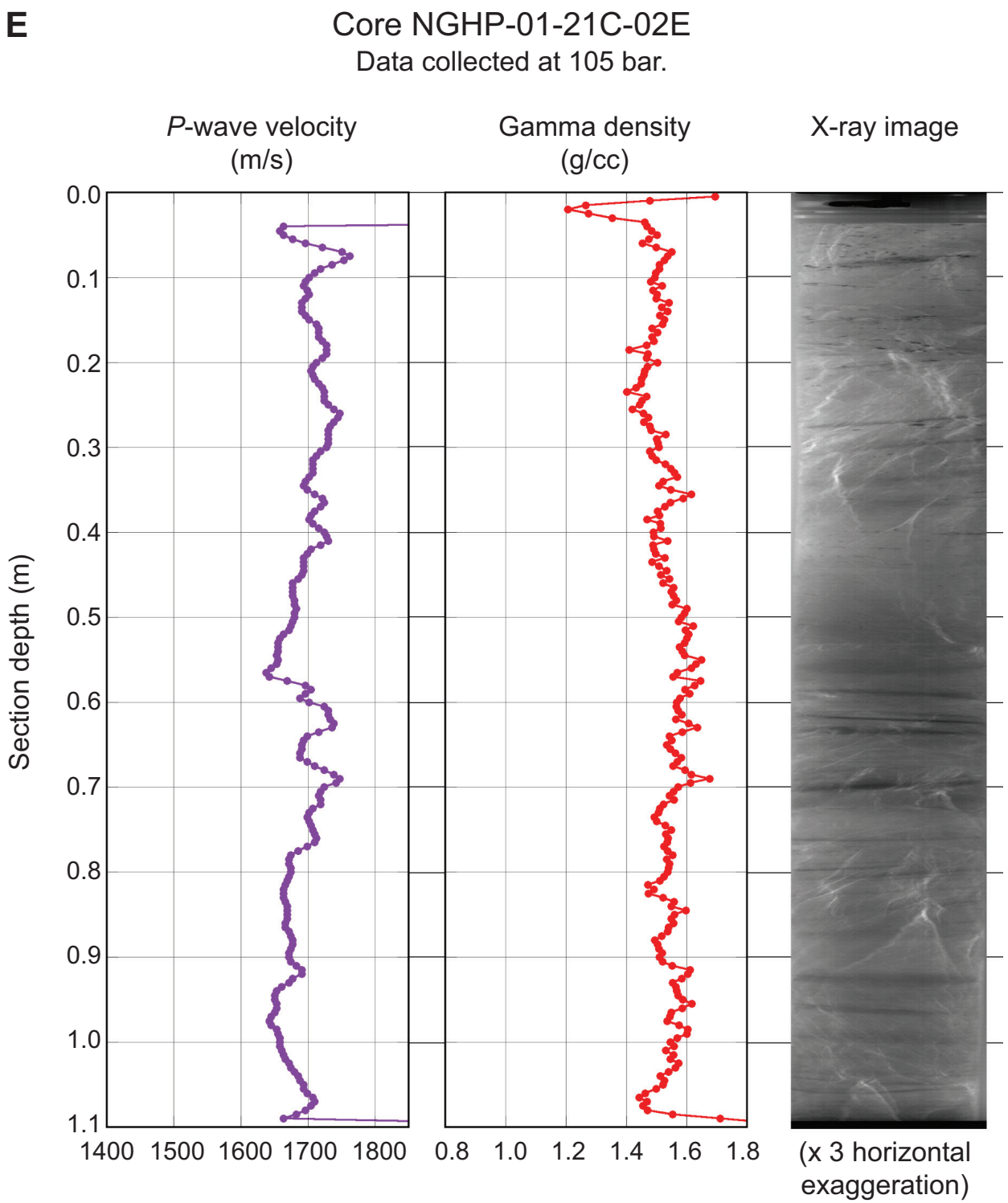

Figure 17. Data collected at near-*in situ* pressure and at 7 °C for successful pressure cores, including X-ray images, gamma density, and *P*-wave velocity. A, Core NGHP-01-21A-02Y; B, Core NGHP-01-21A-03E; C, Core NGHP-01-21A-11E; D, Core NGHP-01-21B-01E; E, Core NGHP-01-21V-02E; F, Core NGHP-01-21C-03Y; G, Core NGHP-01-21C-04E. X-ray images have been stretched 300 percent in the cross-core direction to show detail.—Continued

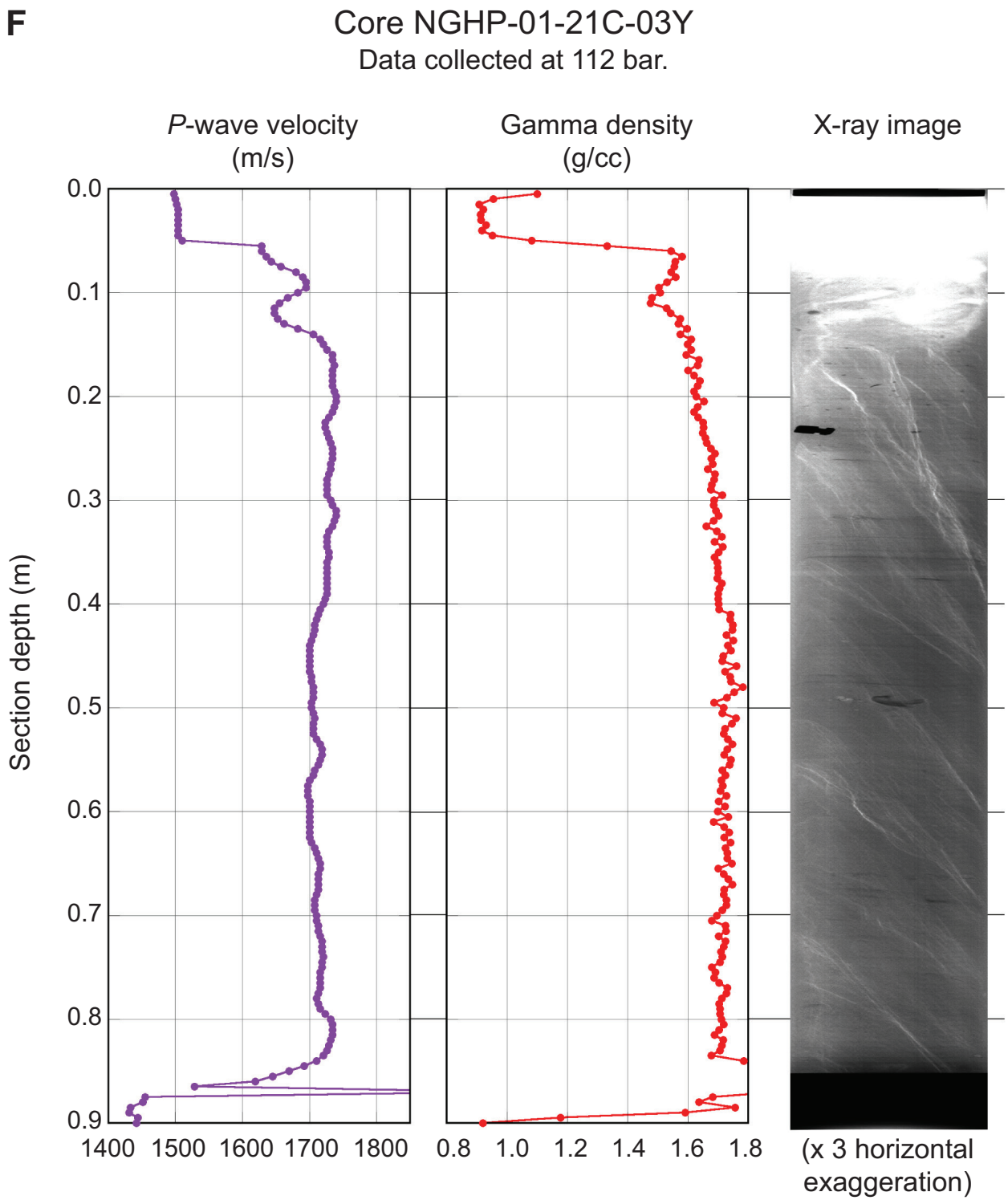

Figure 17. Data collected at near-*in situ* pressure and at 7 °C for successful pressure cores, including X-ray images, gamma density, and *P*-wave velocity. A, Core NGHP-01-21A-02Y; B, Core NGHP-01-21A-03E; C, Core NGHP-01-21A-11E; D, Core NGHP-01-21B-01E; E, Core NGHP-01-21V-02E; F, Core NGHP-01-21C-03Y; G, Core NGHP-01-21C-04E. X-ray images have been stretched 300 percent in the cross-core direction to show detail.—Continued

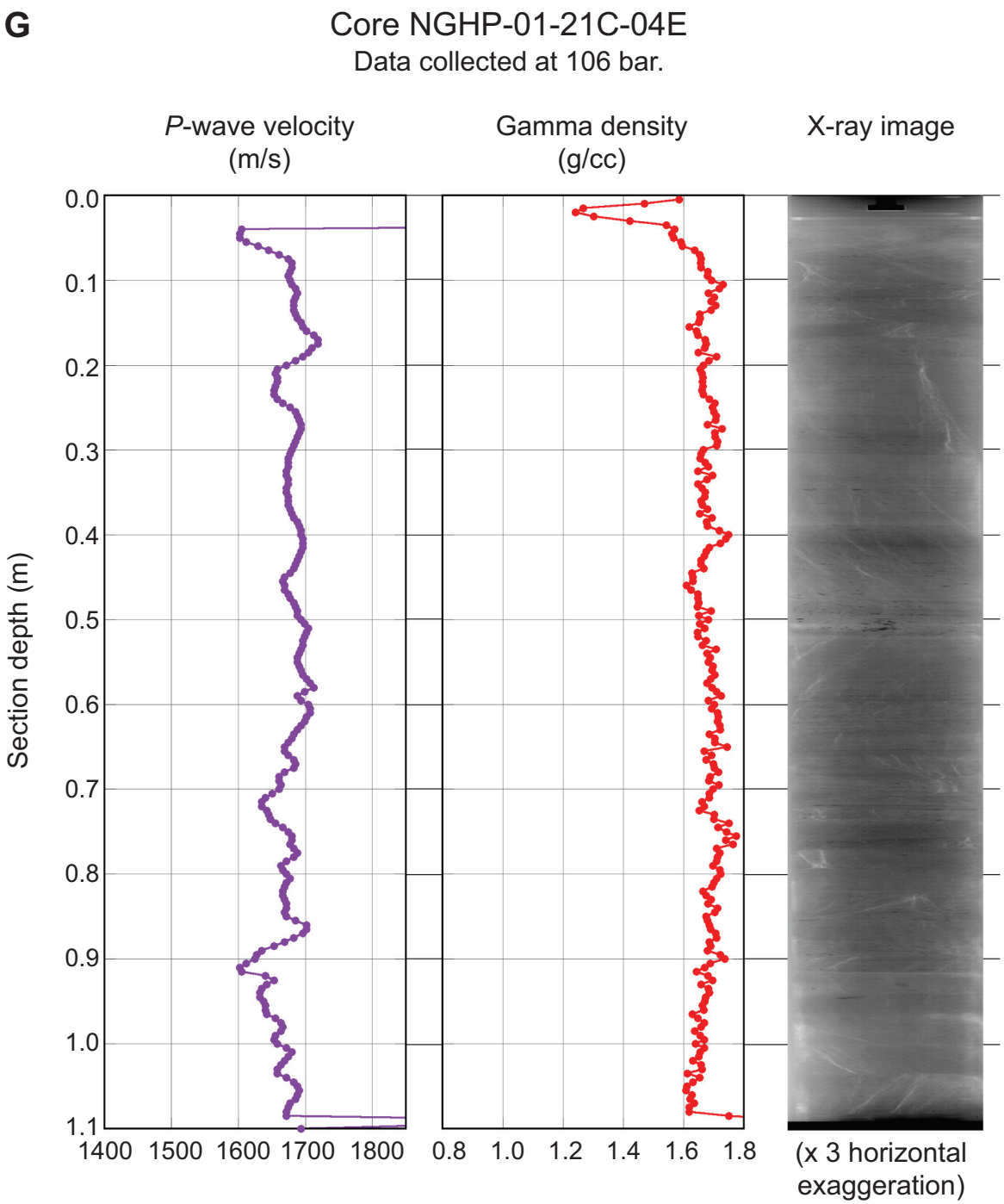

Figure 17. Data collected at near-*in situ* pressure and at 7 °C for successful pressure cores, including X-ray images, gamma density, and *P*-wave velocity. A, Core NGHP-01-21A-02Y; B, Core NGHP-01-21A-03E; C, Core NGHP-01-21A-11E; D, Core NGHP-01-21B-01E; E, Core NGHP-01-21V-02E; F, Core NGHP-01-21C-03Y; G, Core NGHP-01-21C-04E. X-ray images have been stretched 300 percent in the cross-core direction to show detail.—Continued

Table 10. Methane-hydrate volume and concentration in pore space for Core NGHP-01-21A-07E. Values required for calculation of methane-hydrate concentration are also included.

Parameter	Units	NGHP-01-21A-7E
Core diameter	mm	51
Sediment length	cm	109
Sediment porosity	%	57
Pore volume	*liters*	*1.262*
Volume methane collected	liters	68.91
Methane concentration in pore fluids	mM	10.6
Total methane in core	*mmol*	*3009.1*
In situ salinity	ppt	36.0
Methane saturation*	mM	75.6
Methane in pore fluids, assuming saturation	mmol	95.4
Excess methane	*mmol*	*2913.9*
Volume of methane hydrate	ml	397.1
*Methane hydrate, % of pore volume***	*%*	*31.5*

Notes:

Rows in *italics* are calculated parameters.

*Methane saturation calculated from Xu (2002, 2004) using a water depth of 1049 mbsl, a thermal gradient of 46 °C/km (measured for Site NGHP-01-10), a seafloor temperature of 6 °C (measured for Site NGHP-01-10), and the above salinities.

**Assuming all gas hydrate is evenly distributed throughout the pore space.

X-ray images of pressure cores from Site NGHP-01-21 showed gas hydrate in thin, sediment-displacing structures (layers and veins), in massive lumps, and possibly in finely-distributed, grain-displacing forms. Near-horizontal layers were seen in Cores NGHP-01-21A-02Y and -03E. Thin, wispy, subvertical veins were seen in Cores NGHP-01-21A-02Y and -21C-04E. High-angle veins in clusters, which distinctly cross-cut sedimentary bedding, were seen in Cores NGHP-01-21A-03E and -21C-03Y. Massive gas hydrate was seen at the bottom of Core NGHP-01-21A-11E, which showed the highest *P*-wave velocity recorded on NGHP Expedition 01. Indications of finely-distributed, grain-displacing gas hydrate might be seen in the subtle variations in density in the X-ray image of Cores NGHP-01-21A-02Y, -21C-03Y, and -21C-04E. Most cores also showed elevated *P*-wave velocities, either in layers or throughout the core, that could indicate finely-distributed, grain-displacing gas hydrate or gas hydrate disseminated throughout pore space (especially Cores NGHP-01-21A-02Y, -21A-03E, -21C-02E, -21C-03Y, and -21C-04E).

(After the expedition, it was determined that what was originally thought to be disseminated or finely-distributed gas hydrate was actually a network of fine veins, the bulk of which were invisible on the two-dimensional X-ray. See "Singapore Pressure Core Studies" in the Appendix for further discussion.)

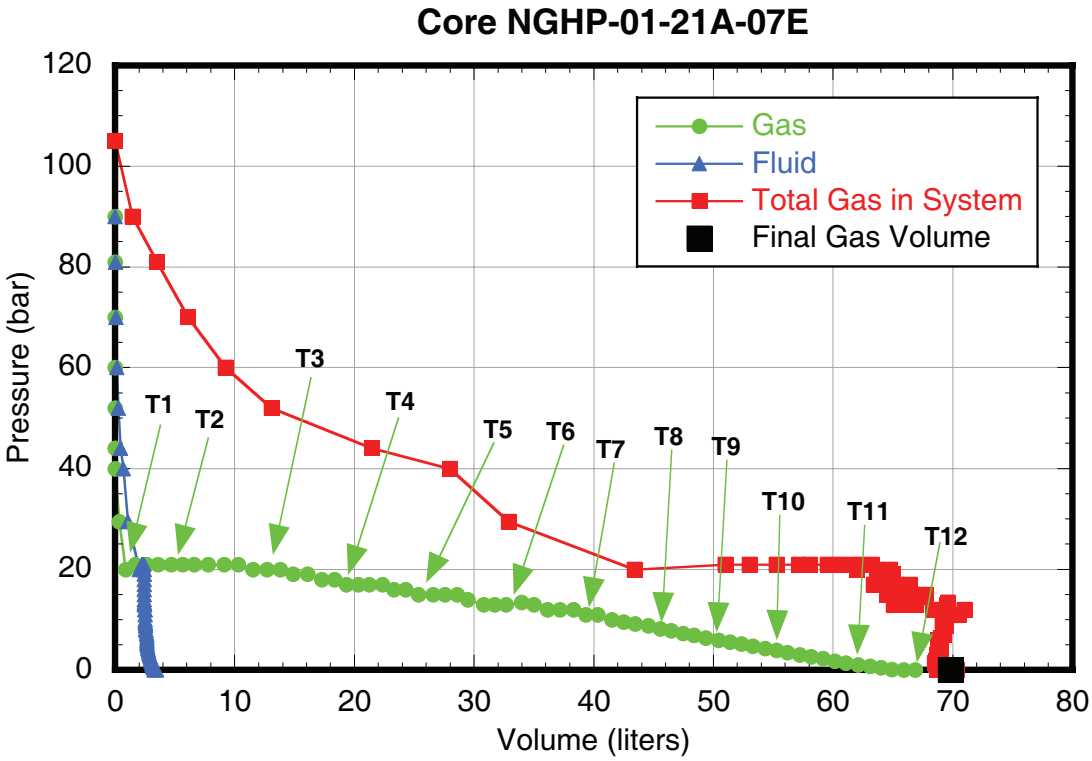

Figure 18. Pressure versus volume for Core NGHP-01-21A-07E, also showing placement of gas samples (see "Organic Geochemistry"). [Green circles, collected gas; blue triangles, collected fluid; red squares, total gas in system (calculated as described in the "Methods" chapter); large black square, final calculated gas from cores; and T (number), gas samples]

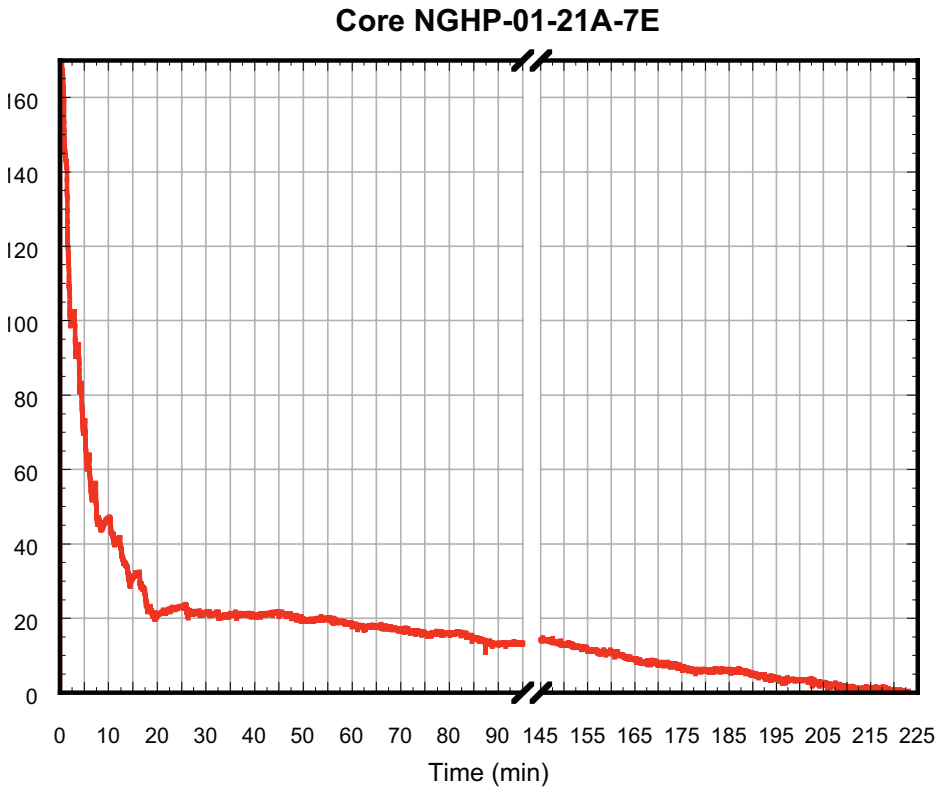

Figure 19. Pressure versus time for Core NGHP-01-21A-07E.

The high-angle gas hydrate veins were particularly interesting, as they appeared to be oriented on a particular plane in the two cores in which they were seen. If the veins are present in only one plane in the core, then it was fortuitous that these cores were imaged in the proper orientation to view them. Similarly, these veins could be present in the other cores at this site, and we could have been merely unfortunate not to have imaged them at the appropriate angle. To determine whether these veins are a feature of all cores at Site NGHP-01-21, the stored cores should be subjected to X-ray tomographic reconstruction or at least should be X-rayed from multiple angles (see "Singapore Pressure Core Studies" in the Appendix for a description of this procedure).

Quality of Cores Stored for Shore-Based Work

Five cores (four from Site NGHP-01-21 and one from Site NGHP-01-10) were stored in HYACINTH storage chambers for shore-based work. These cores are unique, as they have preserved gas-hydrate morphologies in fine-grained sediments at *in situ* pressures and temperatures. They are the best quality gas-hydrate-bearing cores collected on NGHP Expedition 01. Throughout the expedition, the FPC took high-quality, undisturbed cores, as attested to by the well-preserved sedimentological structures (for example, "Lithostratigraphy" in "Site NGHP-01-15") and the lack of seawater infiltration (see "Inorganic Geochemistry" in "Site NGHP-01-19"). While early HRC cores were disturbed by the rotary motion of the drilling, modifications made to the HRC throughout the cruise allowed it to take cores that were of progressively higher quality. The undisturbed bedding and crosscutting gas-hydrate veins in Core NGHP-01-21A-03E are a testament to the improvements.

All five cores were left outside of the gas-hydrate stability zone for as little time as possible during core recovery and contain the greatest number of undisturbed samples of gas hydrate possible to collect at this time. Although the DST Micro data loggers were not used at Site NGHP-01-21 (based on evidence from previous coring runs using these internal data loggers (for example, fig. 37 in "Sites NGHP-01-10, 12, and 13")) the cores experienced up to 10 °C less warming than the tool-data loggers showed (figs. 15 and 16). Therefore, the time the core spent outside of gas-hydrate stability based on the tool-data logger (5–10 min; fig. 16) is overestimated. The rise in pressures that were recorded by the tool-data loggers may indicate minor gas-hydrate dissociation; however, any dissociation that occurred was quickly stopped, as all cores from Site NGHP-01-21 had strong *P*-wave velocity signals. Each of these cores is likely to contain 300–500 mL of gas hydrate, and the amount of gas–hydrate dissociation required to produce a pressure increase of 10–30 bar would be less than 1 mL. Therefore we believe that the gas-hydrate structures and fabrics in these cores are essentially undisturbed.

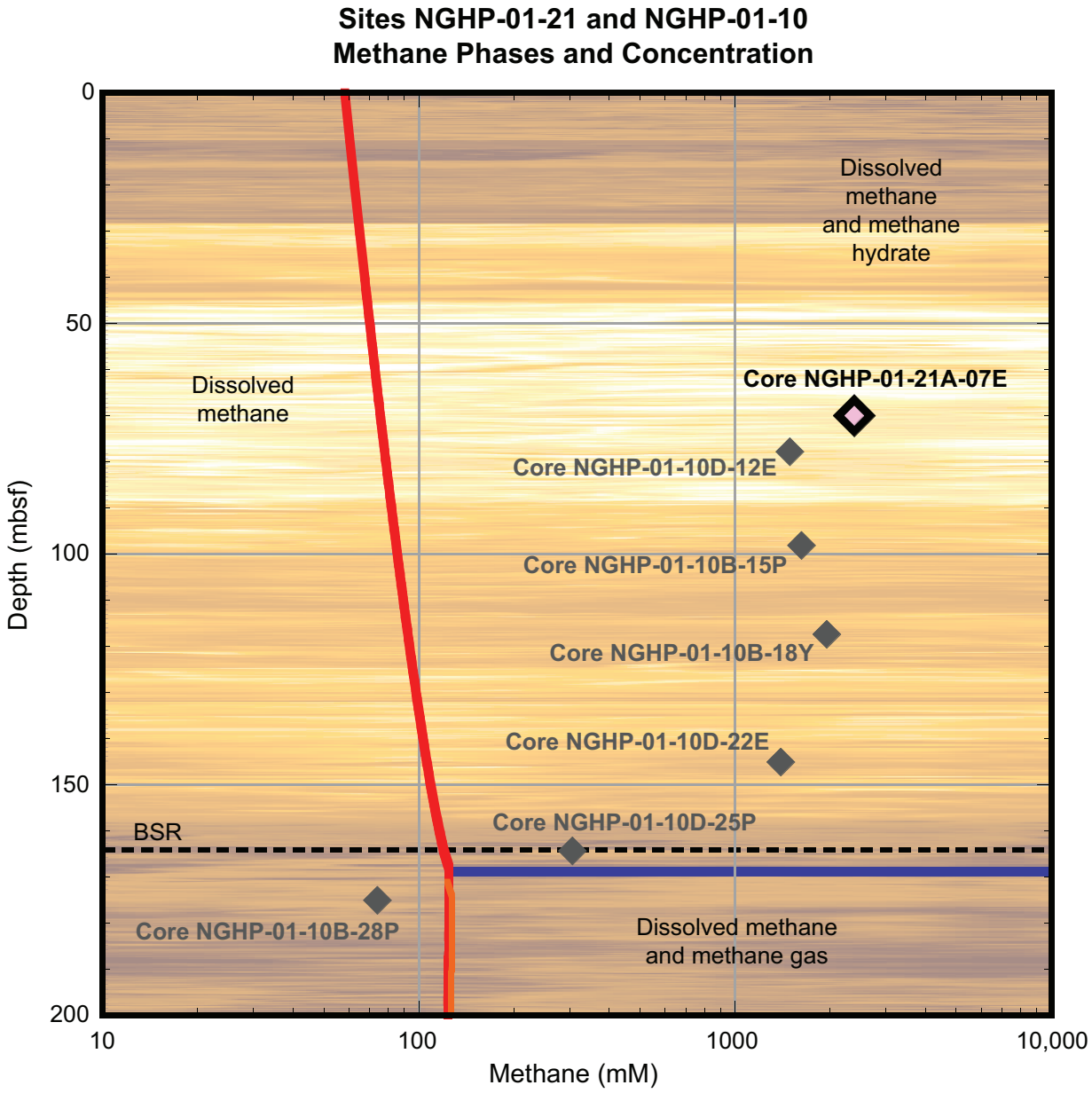

Figure 20. Methane phase diagram for Sites NGHP-01-21 and NGHP-01-10, with total methane concentration measured from Core NGHP-01-21A-07E and the six depressurized pressure cores at Site NGHP-01-10. The shipboard-determined seafloor temperature (6.0 °C) and thermal gradient (45 °C/km) were taken from "Downhole Temperature Measurements" in "Sites NGHP-01-10, 12, and 13." The salinities were the average baseline salinities around the depths of the pressure cores (35 ppt; from table 7), and methane saturation was calculated according to Xu (2002, 2004). The background is the LWD deep-borehole-resistivity (resistivity-at-bit) image for Site NGHP-01-10. [LWD, logging-while-drilling; km, kilometers; ppt, parts per thousand]

Downhole Logging

Operations

After recovering the last pressure core from 1,107 mbrf (57 mbsf), Hole NGHP-01-21B was drilled to the total depth of 1,250 mbrf (200 mbsf) at 0400 hr, 14 August. The hole was then conditioned for logging; it was swept with 30 bbl of sepiolite, displaced with 60 bbl of 10.5 ppg barite, and the pipe was pulled to the logging depth of 1,108.6 mbrf (58.6 mbsf). At 0630 hr, the wireline was spooled and the logging sheaves brought to prepare the rig floor for logging.

Assembly of the triple combo started at 0740 hr. The tool string was complete at 0805 hr, run-into-hole (RIH) at 0840 hr, and reached the bit at 0940 hr. After exiting the pipe without problems, the bottom of the tool could not pass below 1,150 mbrf (100 mbsf) at 0945 hr. After ~20 minutes of fruitless efforts, we decided to bring the tool back to the ship, to clean the hole, and to position the pipe 20 m below this point to get a better chance of logging the deepest part of the hole across the predicted BSR. After failing to reenter the pipe on the first attempt, the drill string had to be raised and rotated by 180° to bring the triple combo fully inside the pipe at 1025 hr. The tool was then brought to the surface at 5,000 ft/hr. It was back on deck at 1020 hr and partially rigged down at 1200 hr.

The hole was washed to total depth, deepened to 1,255 mbrf (205 mbsf), and displaced with 60 bbl of 10.5 ppg barite. After pulling the bit to 1,171 mbrf (121 mbsf), the sheaves and the wireline were repositioned at 1615 hr, and the triple combo was RIH again at 1705 hr. The tool string was at the bit at 1750 hr, and with the assistance of mud circulation to facilitate the exit, it was in open hole at 1800 hr. At 1805 hr, with the cable head only ~10 m below the bit, the bottom of the tool could not pass an obstruction at 1,205 mbrf (155 mbsf). At 1830 hr, after failing to gain more than a few meters, we decided to abort logging operations in this hole and to bring the tool back. At 1835 hr, the top of the tool could not enter the pipe. For the next 2 hr, the drill string was raised and rotated several times, while the unstable formation made it impossible to maneuver the tool underneath. At some point, it was necessary to pull 6,000 lb on the wireline, close to its limit, to disengage the tool from the formation. At 1920 hr, after loosing the head tension and failing to communicate with the tools, it was clear that the wireline was damaged. The triple combo was finally brought inside the pipe at 2055 hr. When it got back to the surface at 2220 hr, the only apparent damage was to the wireline, which was badly spliced and needed to be severed 10 m above the cable head. The tools were cleaned and rigged down at 2300 hr, and the rig floor was ready to pull out of the hole at 0000 hr, 15 August.

No data were properly recorded during any of these aborted runs. However, as the tools were routinely activated a soon as they exited the pipe, the resistivity readings did not show any value that could suggest the occurrence of gas hydrate over any part of the two short sections that were measured.

References Cited

Duan, Z., Møller, N., Greenberg, J., and Weare, J.H., 1992, The prediction of methane solubility in natural waters to high ionic strengths from 0° to 250 °C and from 0 to 1600 bar: Geochimica et Cosmochimica Acta, v. 56, p. 1451–1460.

Xu, W., 2002, Phase balance and dynamic equilibrium during formation and dissociation of methane gas hydrate, *in* 4th International Conference on Gas Hydrates, Yokohama, Japan, 19–23 May 2002, Proceedings: International Conference on Gas Hydrates, p. 195–200,.

Xu, W., 2004, Modeling dynamic marine gas hydrate systems: American Mineralogist, v. 89, p. 1,271–1,279.